A role of vertical mixing on nutrient supply into the subsurface chlorophyll maximum in the East China Sea

李，根淙

A role of vertical mixing on nutrient supply into the subsurface chlorophyll maximum in the East China Sea

Keunjong Lee

January, 2017

A role of vertical mixing on nutrient supply into the subsurface chlorophyll maximum in the East China Sea

A Dissertation
Submitted for the Degree of
Doctor of Science

by

Keunjong Lee

Earth System Science and Technology,
Interdisciplinary Graduate School of Engineering Sciences,
Kyushu University

January, 2017

ABSTRACT

In summer, Changjiang Diluted Water (CDW) expands over the shelf region of the northern East China Sea. Dilution of the low salinity water could be caused by vertical mixing through the halocline. Vertical mixing through the pycnocline can transport not only saline water, but also high nutrient water from deeper layers to the surface euphotic zone. It is therefore very important to quantitatively evaluate the vertical mixing to understand the process of primary production in the CDW region. We conducted extensive measurements in the region during the period 2009−2011. Detailed investigations of the relative relationship between the subsurface chlorophyll maximum (SCM) and the nitracline suggested that there were two patterns relating to the N/P ratio. Comparing the depths of the nitracline and SCM, it was found that the SCM was usually located from 20 to 40 m and just above the nitracline, where the N/P ratio within the nitracline was below 15, whereas it was located from 10 to 30 m and within the nitracline, where the N/P ratio was above 20. The large value of the N/P ratio in the latter case suggests the influence of CDW. Turbulence measurements showed that the vertical flux of nutrients with vertical mixing was large (small) where the N/P ratio was small (large). A comparison with a time series of primary production revealed a consistency with the pattern of snapshot measurements, suggesting that the nutrient supply from the lower layer contributes considerably to the maintenance of SCM.

TABLE OF CONTENTS

1. Introduction

Subsurface chlorophyll maximum is a subsurface maximum in the concentration of chlorophyll in the ocean and it is a common feature in large parts of the tropical and subtropical oceans [*Venrick et al.*, 1973, *Cullen*, 1982, *Letelier et al.*, 2004, *Holm-Hansen and Hewes*, 2004], although there is sometimes more chlorophyll at the surface than at any greater depth. It is generally believed that SCM is a stable feature, depending on seasonal changes in light and nutrient conditions: Light that is supplied from above and nutrients that are often supplied from below. SCM forms close to the boundary where light and nutrient supply allow phytoplankton growth. Especially during the summer season, surface nutrient is completely depleted by consumption of phytoplankton. Strong stratification restrained the nutrient from the lower layer, consequently chlorophyll develops at subsurface rather than surface layer.

Most primary production is presumably within the SCM layer considering the two essential factors. New primary production, utilizing nutrients supplied from lower layer, occurs within the SCM layer [*Hickman et al.*, 2012, *Fernand et al.*, 2013]. Large nutrient input from the continent or large river discharge builds up to the shallow SCM in coastal shelf water [*Chen et al.*, 1999, 2001, *Gong et al.*, 2003, *Liu et al.*, 2010]. Biological production around SCM layer by new supply of nutrients would affect the ecosystem in the shelf sea. For example, enriched nutrient conditions have been observed around the area of high fishery production in coastal seas [*Gong et al.*, 1996, 2000] and upwelling region [*Edmond et al.*, 1985, *Chen*, 1996], where the ecosystem is accelerated by primary production.

The continental shelf region of the East China Sea (ECS) is a biologically highly productive region that is well known as a good fishery and the nursery ground for the larvae of various marine species. It is believed that primary production in the area could be supported by the large amounts of nutrients supplied from the continent of Asia. The shape of the highly productive region, in terms of the horizontal distribution of chlorophyll from satellite observations, tends to resemble that of low salinity water [*Kim et al.*, 2009]. Low salinity water is an indicator of fresh water discharge from rivers, such as Changjiang River.

However, the relatively high chlorophyll region usually extends to the outer shelf or around Cheju Island, where it takes more than 1 month for the materials to arrive from the mouth of Changjiang River. It could be suspected that most of the nutrients from Changjiang River have been consumed by primary production in much shorter time.

An estimation of the nutrient budget in the shelf area of the ECS suggests that the Kuroshio subsurface water could supply more than half of the nutrients entering the shelf region [*Chen and Wang*, 1999]. Therefore, nutrients from the open ocean could play a significant role in primary production in the shelf region, although the estimation by *Chen and Wang* [1999] does not show what proportion of the nutrients from the open ocean could be used for primary production in the shelf region. It is therefore necessary to determine how the nutrients at the subsurface could be transported into the euphotic zone.

The upward transport of high nutrient water residing in the lower layer could be suggested by the dilution process of the low salinity water in the surface layer. *Matsuno et al.* [2010a] showed that salinity increase, namely the dilution of fresh water by sea water, was mostly caused by upwelling as well as vertical mixing generated by the passage of low

5

pressure, at least in regions far from Changjiang River estuary. If the vertical processes, accompanied by strong winds, contribute to nutrient supply into the surface layer and result in primary production there, this would be in opposition to the negative correlation between chlorophyll-a and salinity. Therefore, primary production could occur in a relatively high salinity area.

On the other hand, salinity increase is little under calm conditions [*Matsuno et al.*, 2010b]. It has been suggested that subsurface water would not be transported into the surface layer under calm conditions. Instead, a chlorophyll maximum is often found in the subsurface, beneath the surface mixed layer, suggesting that primary production would occur there using nutrients from the lower layer.

There are many possibilities to supply the nutrients into the surface layer. For example, horizontal transport by strong surface velocity, upwelling from horizontal divergence by strong wind [*Liu et al.*, 1990, *Siswanto et al.*, 2008] and mesoscale eddy dynamics [*McGillicuddy Jr et al.*, 1997, 1998], winter convection in homogenious thermal structure [*Michaels et al.*, 1994], and enhanced vertical mixing within the mixed layer [*Lewis et al.*, 1986, *Crawford and Dewey*, 1989, *McGowan and Hayward*, 1978]. From these mechanisms considerable in the ocean, seasonal SCMs commonly develop in temperate regions when the nutrients are depleted in the surface layer during summer season. Therefore, vertical mixing could be considered as a major mechanism in calm condition to supply the nutrients into the euphotic layer. As turbulent mixing takes place away from boundaries, and a nutrient flux across the isopycnals has long been recognized as an important mechanism for nutrient supply to productive layers in shallow regions [*Crawford and Dewey*, 1989], hence quantification of the nutrient flux driven by vertical

mixing will be helpful to understand the nutrient inputs supplied into the subsurface chlorophyll maximum (SCM) in this region.

How much does the nutrient supply by vertical mixing contribute to primary production in the shelf region of ECS, putting aside the terrestrial nutrients from Changjiang River? Quantitative estimates of vertical nutrient flux through direct turbulence measurements have rarely been reported in this region (Fig. 1.1). For example, new production by vertical nitrate flux is derived from stability using the empirical equation [*Kwak et al.*, 2013] or nitrate assimilation method including nitrogen source of advection and atmospheric input [*Chen et al.*, 1999]. From the other reports using direct measurements, either the measured area is restricted to the continental slope far away from the shelf region influenced by Changjiang River [*Liu et al.*, 2013], or the suggested values are instantaneous and do not consider the large variability of vertical nutrient flux during the day [*Shiozaki et al.*, 2011].

Our study area is influenced by two major nutrient sources; Changjiang diluted water (CDW) with relatively nitrate rich water and Kuroshio subsurface water (KSSW) with relatively phosphate rich water. The nutrients which is found in phytoplankton and throughout the deep oceans keep relatively consistent ratio, which is empirically found to be Carbon:Nitrogen:Phosphorus (C:N:P) = 106:16:1, known as the Redfield ratio. The Changjiang River discharge has a large N/P ratio, for example, 46-84 reported by *Edmond et al.* [1985], *Zhang* [1996], and would gradually decrease the N/P ratio through the mixing with the shelf water, while it would still higher than the Redfield ratio of 16 in the CDW. In contrast to the high N/P ratio found in CDW, the N/P ratio of KSSW is slightly lower than the Redfield ratio of 16 [*Liu et al.*, 2000] in the subsurface water on the shelf, where

the N/P ratio could be reduced by regeneration of phosphate from the sediment. Thus, there are two types of nutrient sources also in a viewpoint of the N/P ratio. Consumption by phytoplankton could enhance the N/P ratio increase/decrease in the high/low N/P ratio water. Nevertheless, it is expected that continuous nutrient input from the different N/P ratio water can determine the N/P ratio in the nitracline. Therefore, the N/P ratio would be effective to discriminate the nutrient supply from the CDW and/or KSSW.

In this study, we examined the nutrient flux by vertical mixing associated with the N/P ratio and quantified the contribution of vertical nutrient flux to the SCM based on the direct measurements of turbulence. We improved the reliability of the vertical nutrient flux using massive amounts of data, including many snapshots and time series measurements. Simultaneous measurements of primary production were also made to determine the contribution of the vertical nutrient flux to primary production around the SCM.

The structure of this thesis is as follows.

In section 2, we describe the observations in general. Intensive measurements were conducted in the region southwest of Jeju Island during the period 2009−2011 including two time series measurements in each year. The methods estimating vertical nutrient flux and primary production are also described in detail.

In section 3.1, we show the horizontal expansion of CDW which is considered as one of the main nutrient sources and describe the formation and depth of SCM relating to the influence of CDW.

In section 3.2, detailed investigations of the relative relationship between the depths of SCM and nitracline suggest that there were two patterns relating to the N/P ratio which could be considered as an indicator originating from different nutrient source.

In section 3.3, the results of estimating vertical nutrient flux and primary production are described in detail. Turbulence measurements show that the vertical flux of nutrients with vertical mixing and its contribution to primary production in the vicinity of the SCM were large (small) where the N/P ratio was low (high). The former case indicates a significant nutrient input from the lower layer.

Meanwhile, large variability of vertical nutrient flux exaggerates their mean contribution to primary production in case of low N/P ratio. The snapshot measurement includes some uncertainty about representing daily mean flux, therefore, we try to evaluate the vertical nutrient flux by using the time series measurements in section 3.4. Due to the lack of nutrients data in the time series, we use the linear relationship between the temperature and nutrient concentrations below the nitracline. An estimation using the time series measurements lessened the variability of vertical nutrient flux as well as revealed a consistency about large contribution of vertical nutrient flux to primary production in case of low N/P ratio with the same pattern of snapshot measurements.

In section 4, we discuss on the cause of observed turbulence, another physical processes providing nutrient supply, uncertainties in the estimation of vertical nutrient flux and primary production, and consistency of vertical eddy diffusivity. Especially, statistical approach supported the significance of difference of vertical nutrient flux between the case

of low and high N/P ratio, even allowing for the daily large variation of vertical eddy diffusivity.

Finally, in section 5, we conclude that, despite some uncertainties estimating vertical nutrient flux and primary production in the vicinity of SCM, the nutrient supply from lower layer associated with the vertical mixing contributes considerably to the maintenance of SCM.

Figures
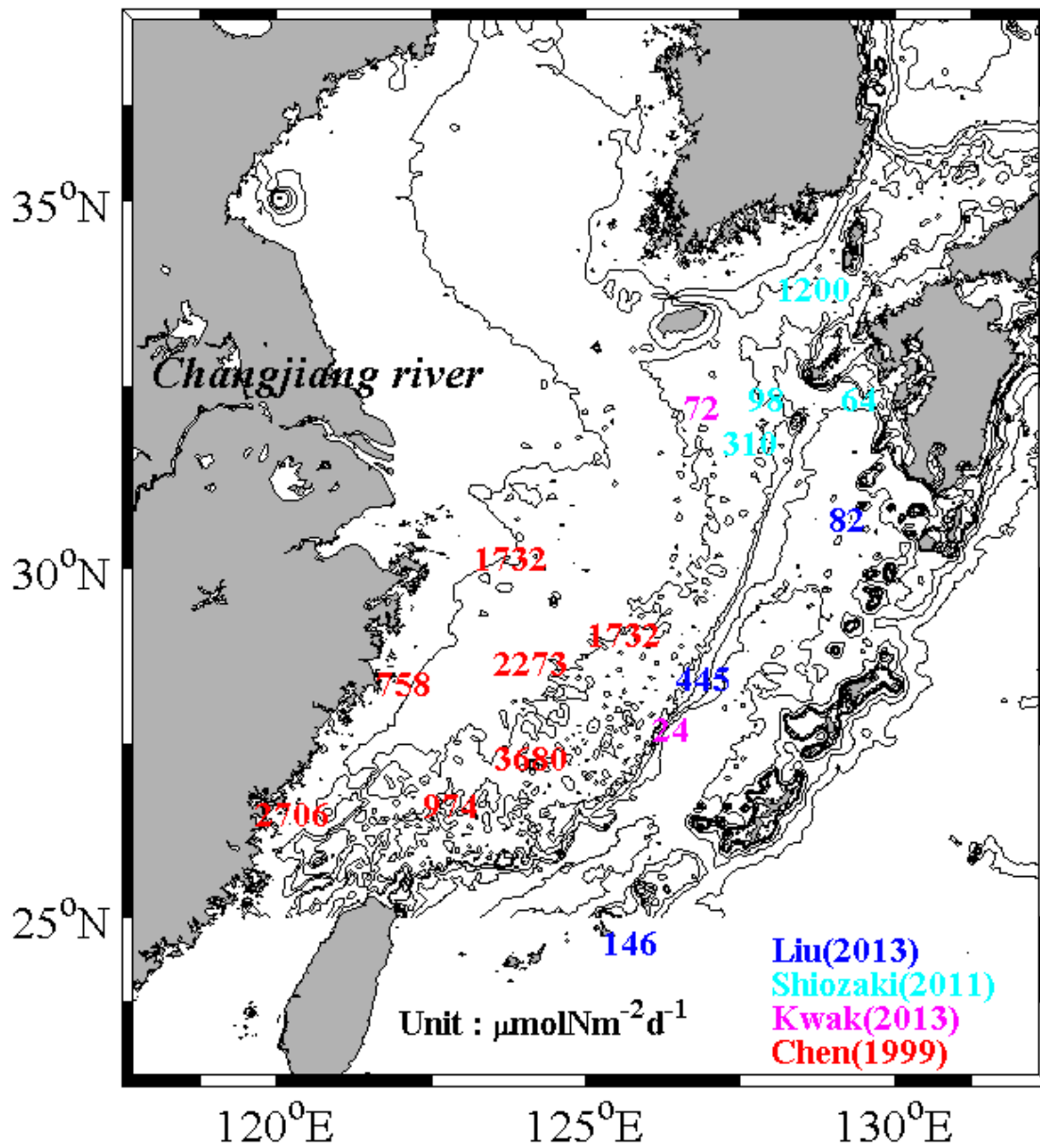
Fig. 1.1 Reported new production by vertical nitrate flux in the East China Sea.

2. Observations and methods

2.1. Study area

The ECS is a marginal sea surrounded by the Eurasian continent and a chain islands. Most of the area of the northern ECS is shallow (<200 m) continental shelf, but the deep Okinawa Trough is (>1000 m) located in the eastern and southeastern ECS. The summer monsoon usually drives the CDW southeastward or eastward across the shelf region [*Chang and Isobe*, 2003]. A strong western boundary current, the Kuroshio originates from bifurcation of the North Equatorial Current east of the Philippines in the North Pacific Ocean, and a main branch of the Kuroshio flows northward through the Okinawa Trough. It finally bifurcates to the east through the Tokara Strait and another branch flows northward along the west of Kyushu. The area of observation was the southwest of Cheju Island, with most of the area being inside the Korean EEZ.

Physical and biochemical measurements were made in the northern ECS onboard the Nagasaki-maru, a training ship of Nagasaki University, during cruises N-286, N-309, and N-333 in July 2009, July 2010, and July 2011, respectively. The location of observations is shown in Fig. 2.1. The observation area generally consisted of four zonal sections (from the north: KD, KC, CLON, and CK-sections) and one meridional section (MD-section). The observation sections were slightly adjusted to match the detailed cruise plan in each year. The numbering of stations on each zonal section started from the east; on the meridional section, numbering started from the north.

2.2. Hydrography

Hydrographic observations were conducted using a CTD (SBE 9plus manufactured by Seabird Electronics, Inc.) attached with a chlorophyll fluorometer (Seapoint chlorophyll fluorometer manufactured by Seapoint sensors, Inc.), which was lowered to about 5 m above the bottom.

2.3. Turbulence

Measurements of microstructure, i.e., the small-scale vertical shear of the current velocity, were conducted with a microstructure profiler, TurboMAP manufactured by JFE Advantech. The profiler was also equipped with temperature and fluorescence sensors. TurboMAP falls freely to the bottom with a sinking speed of about 0.5 m s^{-1}, with a guard protecting the sensors. Turbulence measurements using the TurboMAP with concurrent CTD observations were conducted at 20 stations, occasionally with successive observations for longer than 24 hours. The profiler was repeatedly cast two or three times at each station and during successive observations. The shape of the shear spectra was approximately fitted with the Nasmyth's universal spectrum, as shown in Fig. 2.2. Thereafter, consecutive profiles were averaged to one ensemble data after omitting abnormal data that did not fit the Nasmyth spectrum [*Nasmyth*, 1970].

Using the vertical microstructure profiles, we calculated the dissipation rate of turbulent kinetic energy ε. All data were sampled at 512 Hz and ε was determined with a sliding window of 1536 data points. The ε was calculated by integrating the small-scale shear spectrum with the wave number and was used by linear interpolation every meter. The detailed calculations of ε are described in *Endoh et al.* [2014]. The vertical eddy diffusivity K_z was calculated from ε and the buoyancy frequency N using $K_z = \Gamma \varepsilon / N^2$

[*Osborn*, 1980]. The mixing ratio, Γ, was set to 0.2 [*Oakey*, 1982]. Data shallower than 10 m were removed due to unstable movement of the instrument shortly after its release.

2.4. Nutrients

To measure the concentrations of nutrients and chlorophyll a, water samplings were made in general at 0, 10, 20, 30, 40, 50, 75, 100, 125, 150, and 5 m from the bottom (varying with the water depth) in addition to the depth of SCM using Niskin bottles mounted on a Rosette sampler (General Oceanics, Inc.) with a CTD probe (SBE 9/11, Seabird Electronics, Inc.). The detailed sampling methods of nutrient concentrations were described in *Umezawa et al.* [2014].

2.5. Chlorophyll a

It is required to know the fine structure of chlorophyll a concentration rather than the ordinary 10 m interval of CTD sampling for the better estimation of primary production around the SCM. To acquire high resolution vertical profiles of chlorophyll a, fluorescence measured with CTD and TurboMAP measurements were used following the calibration of fluorescence data with the chlorophyll a concentration from water sampling. The measured fluorescence by CTD and TurboMAP had a good correlation with the sampled chlorophyll a concentration, with a high correlation coefficient (R > 0.81) in most linear regression analyses (Table 2.1).

2.6. Method for estimating vertical nutrient flux

We made an estimate of the nutrient supply by vertical mixing within the nitracline. There are various ways to determine the passage of nutrient flux into the SCM. To define the vertical gradient of nutrient to calculate the nutrient flux, some studies suggest the use

of gradient intervals in which the largest nutrient gradient occurs [*Hales et al.*, 2005], while

others suggest the use of base of the mixed layer [*Schafstall et al.*, 2010] or a specific

isopycnal [*Sharples et al., 2007*; *Williams et al.*, 2013]. Here we used the layer in which

the largest nitrate gradient was found to calculate the vertical nutrient flux.

The vertical nutrient flux caused by turbulence mixing was calculated by

multiplying vertical eddy diffusivity with the vertical gradient of nutrient concentration

using Fickian diffusion theory, $F = -Kz\, \partial C/\partial z$ (Fig. 2.3). Vertical eddy diffusivities for

the flux calculation were determined by arithmetically averaging K_z values from all

available microstructure casts at each station within the nitracline. For three stations, G1 in

2010, and CK6 and G1 in 2011, where we repeated consecutive observations every hour

for more than 24 hours, K_z was determined as a daily mean.

2.7. *Method for estimating primary production*

The daily primary production integrated within the euphotic zone (IPP) was

calculated to compare the nutrient supply caused by vertical mixing using the following

equation.

$$IPP = \int_{t=0}^{D} \int_{z=0}^{Zeu} B(z) P^{B}(z,t)\, dzdt\,,$$

where D is length of the day, Z_{eu} is euphotic depth, P^{B} is the photosynthetic rate, B

is the chlorophyll a biomass, which was determined with fluorescence measurements made

by the fluorometer attached on CTD and TurboMAP and calibrated with an analysis of

sampled water. Because it is inappropriate to compare the nutrient flux directly with IPP,

which includes a large portion of surface vigorous primary production, we estimated the

integrated primary production within the vicinity of SCM (IPPS) to compare the nutrient flux with their contribution to the primary production around the SCM. We integrated from the euphotic depth to just above the SCM, where chlorophyll concentration is 0.8 times higher than the maximum chlorophyll concentration to avoid the inclusion of surface primary production. The P^B was determined using the data of a *Diving Flash* FRRF (Fast Repetition Rate Fluorometry) manufactured by Kimoto Electric. The detailed methods are described elsewhere in *Mino et al.* [2014]. Because snapshot measurement did not cover the whole day, to calculate the daily primary production, photosynthetic parameters (α, β and P^b_{max}) used to fit the P-I curves were estimated with following formulae suggested by *Platt et al.*, [1980].

$$P^B(z,t) = P^B_{\max}\left[1 - \exp\left(\frac{-\alpha E(z,t)}{P^B_{\max}}\right)\right]\exp\left(\frac{-\beta E(z,t)}{P^B_{\max}}\right),$$

The parameters α, β and P^B_{max} represent the initial slope characterizing the photochemical reactions of photosynthesis, the negative slope characterizing the photoinhibition process and the maximum chlorophyll a normalized photosynthetic rate of the Photosynthetic-Irradiance curve (P-I curve), respectively. $E(z,t)$ is the availability of photosynthetically active radiation (PAR) at depth z and was estimated from the Lambert-Beer law [$E(z,t)=E(0,t)\exp(-kz)$]. $E(0,t)$ was estimated through daily measurements of PAR using a Biospherical Instruments QSL (Quantum Scalar Laboratory Sensor manufactured by Biospherical Instruments Inc) during each cruise, then roughly converted to the irradiance just beneath the surface by multiplying by 0.9 [*Marra*, 2014]. The daily cycle of 30 min moving-averaged incident PAR resembled a sinusoidal curve, hence we estimated the daily variation of PAR empirically using a cubic sine function in the absence of PAR

measurements (July 21, 2009, Fig. 2.4). The vertical attenuation coefficient k was obtained by linear regression from the log-transformed underwater irradiance profile.

Meanwhile, the nutrient (nitrate, phosphate) fluxes were converted to nitrate-based PP (PP-NF) and phosphate-based PP (PP-PF) by multiplying the Redfield ratio and carbon atomic mass. The IPP was converted to net primary production, which includes new and regenerated primary production by multiplying by 0.9 [*Epply and Renger*, 1986, *Yoon et al.*, 2012] to exclude the respiration by phytoplankton. We found that FRRF measured IPP was overestimated with the measured IPP from ^{13}C incubation method at two stations (G1, 2010 and 2011). The ratio of FRRF derived IPP and measured IPP is around 2.8, which gives similar to deducing that P^B from the modelled FRRF was approximately 3-fold higher than the measured P^B [*Mino et al.*, 2014]. Thus, in this study, all the FRRF derived IPP was divided by 2.8 to get reasonable agreement with in situ measurement results.

Tables

Table 2.1 Calibration results between chlorophyll a concentration from the water sampling and fluorescence measured by CTD and TurboMAP. A correlation equation is derived from the linear regression using the least square method. Y is directly measured chlorophyll a concentration from the water sampling. X is fluorescence measured by CTD and TurboMAP.

| Station	Correlation equation	Correlation efficient
MD7, '09	Y = 0.9298X	0.99768
MD5, '09	Y = 1.1853X	0.99450
MD3, '09	Y = 1.2441X	0.91652
MD1, '09	Y = 1.4990X	0.81912
CLON7, '09	Y = 1.5665X	0.99954
CLON5, '09	Y = 1.3525X	0.89988
CLON3, '09	Y = 1.3848X	0.99549
CLON1, '09	Y = 1.2666X	0.98016
MD7, '10	Y = 1.5824X	0.85095
MD5, '10	Y = 2.4178X	0.87433
MD3, '10	Y = 1.2805X	0.86808
MD1, '10	Y = 2.6286X	0.96043
CLON4, '10	Y = 1.8255X	0.81860
KD2, '10	Y = 1.5689X	0.98901
G1, '10	Y = 1.9343X	0.99211
B3, '10	Y = 1.2656X	0.97222
CK6, '11	Y = 1.1940X	0.89277
MD3, '11	Y = 1.7570X	0.96196
MD4, '11	Y = 1.1355X	0.94218
G1, '11	Y = 1.5071X	0.52855

Figures
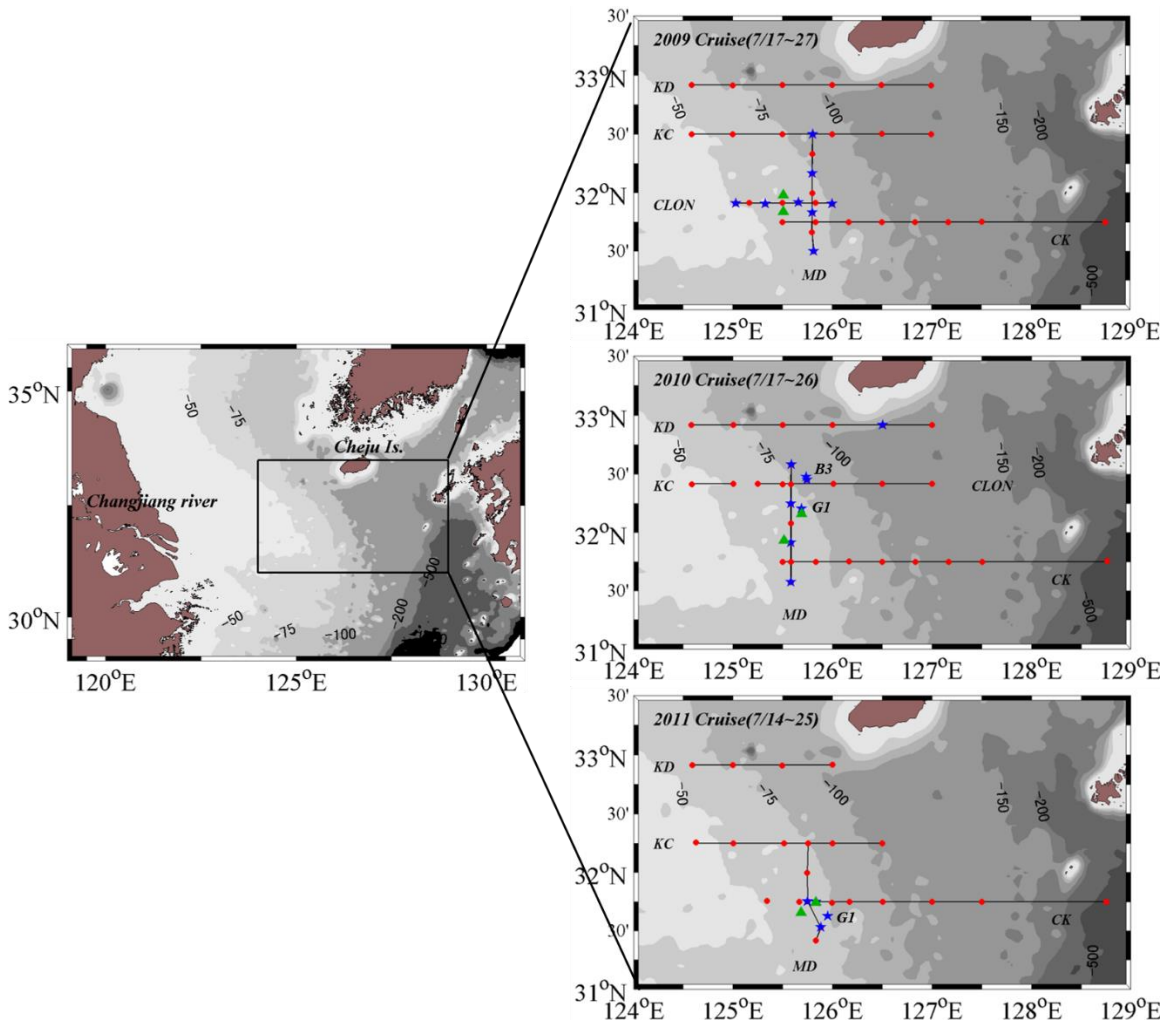
Fig. 2.1 Map of the study area (left) and an enlarged view of the observation sections in 2009, 2010, and 2011 (right). The observation area consisted of four zonal sections (KD, KC, CLON, and CK) and one meridional section (MD). A number of stations on each section was assigned from east to west (east-west section) and from north to south (north-south section). A blue star indicates that CTD and TurboMAP measurements were conducted concurrently. A green triangle indicates that time series measurements were conducted. The locations of G1 (2010 and 2011), B3 (2010) are highlighted as inserting a

text right to the symbol. The locations of G1 and B3, 2010, and G1, 2011 are 125°41.47'E, 32°12.37'N, 125°44.00'E, 32°28.66'N and 125°57.06'E, 31°37.57'N, respectively.
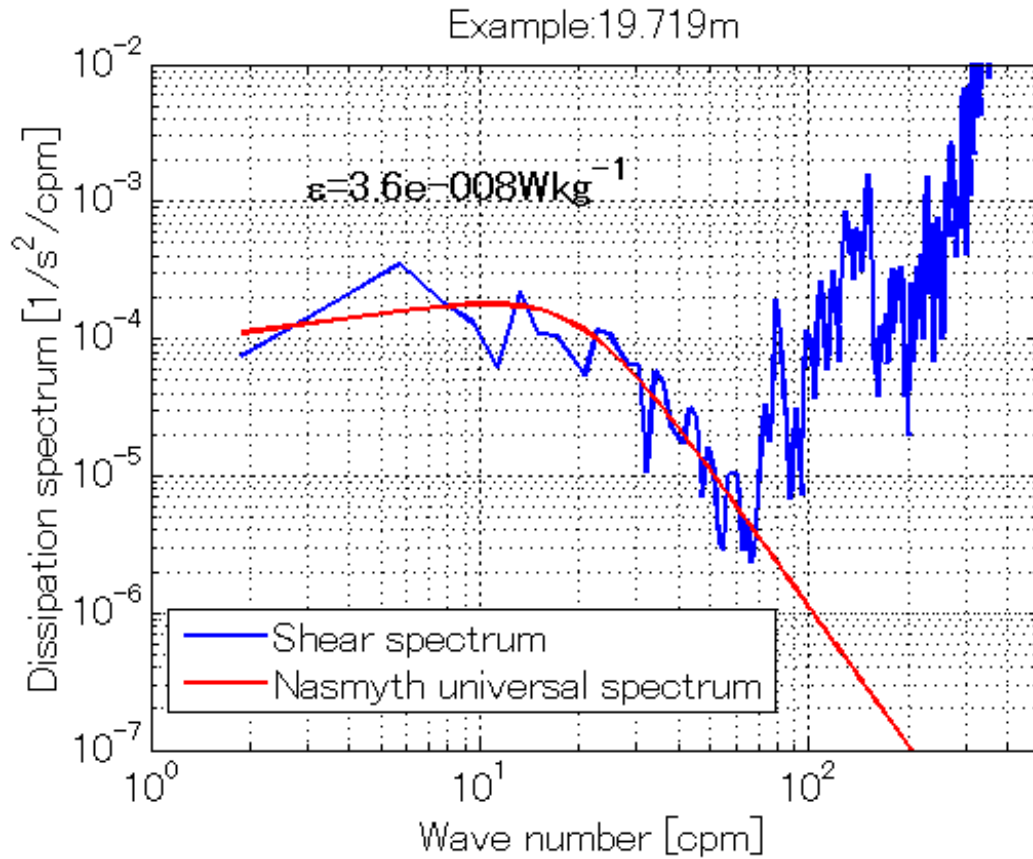
Fig. 2.2 An example of shear spectrum obtained during observations at MD7, 2009. The red line is the Nasmyth universal spectrum corresponding to the shown value of ε. The dissipation rate ε is computed by integrating the measured shear spectrum from 1 cpm to the highest wave number not contaminated by vibration noise.
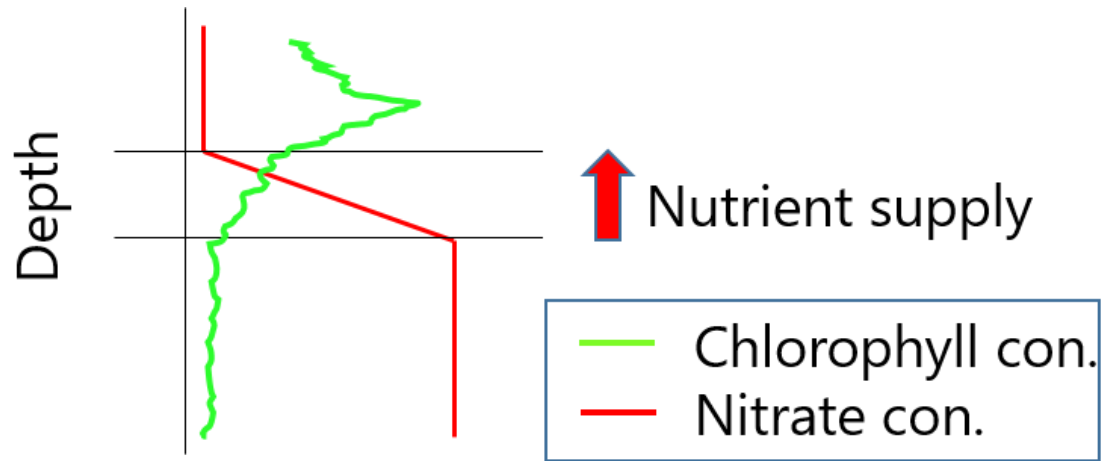
Fig. 2.3 Vertical profiles of chlorophyll (green) and nitrate (red) concentrations. Nutrient supply into the SCM is depicted by vertical mixing through the nitraline. Nitracline is assigned to nitrate gradient higher than 0.25 mmolm^{-4}.
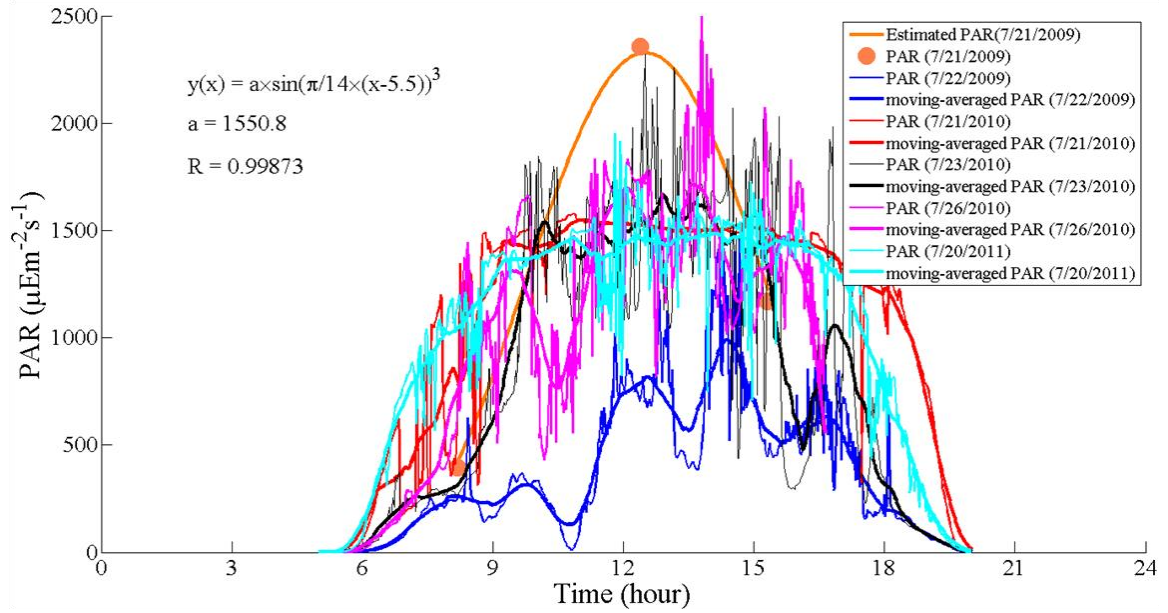
Fig. 2.4 PAR variations during the day of turbulence measurements. Thin and Thick line indicates to measurements of PAR and 30 minutes moving averaged PAR, respectively. The orange circles are PARs of CTD measurement available in Jul. 21, 2009 and orange line is fitted to raw PAR using the sinusoidal curve ($y=a\times\sin[\pi/DL(x-b)]^3$) , DL and b is the length of day and axial migration, respectively. In here, we used 14 and 5.5 hours to DL and b.

3. Results

3.1. *Horizontal structure of hydrography regarding nutrients sources*

Three or four east-west transect observations were conducted repeatedly in 2009, 2010, and 2011, roughly along the pathway of CDW expansion. The profiles of salinity, nutrients, and chlorophyll a along the transect sections usually had a similar vertical structure every year, showing the influence of CDW. The profiles differed slightly depending on greater or lesser expansion of CDW. Typical vertical structures of salinity, density, and fluorescence calibrated with the chlorophyll a, nitrate, and phosphate concentrations, are depicted according to CDW expansion in two horizontal sections, KC and CK, 2009 (Fig. 3.1). The two parallel transects displayed some discrepancies in their vertical structure.

In the southern section (CK-transect in 2009), the salinity of surface water was less than 32 psu and a slight influence of fresh water remained throughout the CK-transect. The strong stratification located around 20 m lay between CK5 and CK2, while the stratification was weak on the eastern side of the CK-transect, west of Kyushu (Fig. 3.1d). Nitrate in the upper layer (< 20 m) was depleted throughout the CK-transect, except for CK6. Chlorophyll a concentrations were high with a sharp maximum (> 3 mgm^{-3}) on the western side of the CK-transect, whereas they were low with a deep and gentle maximum (< 1.5 mgm^{-3}) on the eastern side (Fig. 3.1f).

In the northern section (KC-transect in 2009), remarkably low salinity water (< 30 psu) extended eastward to the south of Jeju Island. Surface low salinity water usually enhanced a strong stratification in the summer. A significant pycnocline existed between

20 to 30 m throughout the KC-transect (Fig. 3.1c). Nitrate in the upper layer was mostly depleted (< 0.1 mmolm^{-3}), except for the western end of the transect. Surface nitrate concentrations higher than 2 mmolm^{-3} were measured at KC6. Phosphate concentrations higher than 0.2 mmolm^{-3} were also found at the western end of the transect. When comparing the concentration of nitrate and phosphate in accordance with the Redfield ratio, nitrate was found to be richer than phosphate at the surface in the western part of the transect and in the layer between 20 to 30 m within CDW expansion, while phosphate was richer than nitrate below 40 m in most locations. Generally, chlorophyll a levels less than 2 mgm^{-3} were distributed above 20 m along the KC-transect. Surface chlorophyll a concentrations were high, with a gentle maximum of chlorophyll a (< 2 mgm^{-3}), i.e., the SCM was not distinctive while it was within CDW expansion.

3.2. *Relative positioning of SCM depending on the N/P ratio*

We collected data of nutrient concentration from the water sampling with CTD observation. The measured N/P ratio is shown in Fig. 3.2 with ordinary water sampling depth. The distribution of N/P ratio consists of two features according to the criterion of the Redfield ratio (N:P = 16:1). The low N/P ratio less than 16 appears beneath 40 m, which is considered as influence of the KSSW and shelf water above the bottom. While, in the layer of 10 ~ 30 m, there exists the high N/P ratio much higher than 16, which is considered as influence of the CDW. Focusing on the layer of 10 ~ 30 m, where the nitracline and SCM are frequently formed at this observed area, two different waters are mixed and it is hard to mention which is dominant. Thus, the N/P ratio would be effective to discriminate the nutrient supply originated from the CDW, and KSSW or shelf water above the bottom.

We inspected profiles of salinity, nitrate, chlorophyll a, and vertical eddy diffusivity to determine the relationships of the relative positioning of the layers with these variables under low and high N/P ratio conditions. Each profile is presented individually for the two conditions: LNP (Fig. 3.3a) and HNP (Fig. 3.3b), where the N/P ratio within the nitracline was less than 15 and larger than 20, respectively. The nitracline was regarded as the layer of 10 or 20 m thickness where the largest nitrate gradient occurs.

The thickness of the surface mixed layer was about 10 m for HNP (Fig. 3.3b) and less than 15 m for LNP (Fig. 3.3a). A strong halocline was present in the nitracline for LNP, while the gentle gradient of salinity for HNP indicates that surface and subsurface water was likely to be mixed, except for stations MD1, MD3, and B3 (2010). A shallow SCM appeared within 10 m at the three stations where strong haloclines were found. Each chlorophyll a maximum varied in shape, but had similarities in positioning related with the nitracline. The SCM was located just above the nitracline for LNP and within the nitracline for HNP.

Vertical eddy diffusivity is a function of the turbulent dissipation rate and buoyancy frequency. Hence, vertical diffusion is enhanced by strong turbulence or weak stratification. Relatively large salinity gradient observed within the nitracline at HNP presumably enhanced the density stratification; as a result, vertical eddy diffusivity did not exceed 10^{-5} $m^2 s^{-1}$ in the nitracline. On the other hand, the salinity gradient within the nitracline was usually small at LNP and the vertical eddy diffusivity occasionally exceeded 10^{-4} $m^2 s^{-1}$.

The depth of the SCM was positively correlated with the depth of the nitracline and pycnocline, strictly speaking, the upper boundary of the nitracline and the lower boundary

of the pycnocline using the data combined from all CTD stations (Fig. 3.4a, b). The lower boundary of the pycnocline was defined as the depth, where potential density is lower than 0.2 kg m^{-3} compared to a reference value at 6 m above the bottom. The relevance of the relative positioning of these hydrographic conditions has been reported [*Kononen et al.*, 1998; *Williams et al.*, 2013], and was also apparent from the vertical profiles discussed before two paragraphs (Fig. 3.3).

The relationship between the relative positioning of the SCM and the nitracline is meaningful. The vertical position of the SCM was mostly in a range between 20 to 40 m and was located slightly above the upper boundary of the nitracline, where the N/P ratio was below 15 within the nitracline, LNP. This positioning of the SCM relative to the nitracline suggests that nitrate, for the production of the SCM, could be supplied from the lower layer. Similar results for the vertical positioning of the nitracline and SCM have been reported by *Shiozaki et al.* [2011]. On the other hand, the vertical position of the SCM was mostly between 10 to 30 m in shallower waters and was located at the interior of the nitracline, where the N/P ratio was above 20, HNP (Fig. 3.4a). The vertical range of the SCM was likely to be within the layer of CDW expansion and nitrate was not derived only from the supply from the lower layer.

On the other hand, the vertical position of the SCM was highly correlated with the depth of pycnocline (Fig. 3.4b). This seems to be related to the small vertical eddy diffusivity, which subsequently leads to an insufficient nutrient supply from lower layers due to the large buoyancy frequency in the lower part of the pycnocline. The SCM is shallower than the lower boundary of the pycnocline in high N/P ratio water. This implies

27

that the existence of nutrient pathways other than from the lower layer, as discussed in the previous paragraph.

The combined distributions of nitrate and salinity for all profiles from 2009 to 2011 are shown together with the N/P ratio (Fig. 3.4c) and sampling depth (Fig. 3.4d). A hypothetical line was assumed to discriminate the nutrient-devoid saline water from the nutrient-laden low salinity water proposed in the Changjiang estuary, with a slope of -4.6 mmolm^{-3}/psu [*Zhang*, 1996]. Nitrate-rich (> 5 mmolm^{-3}) and high salinity (> 32.5 psu) water was found in the deeper layers (> 40 m) above the mixing line, while surface water (< 20 m) was mainly composed of proper nitrate-reservoir water, which had a negative relationship with nitrate and salinity [*Gong et al.*, 2000; *Lie et al.*, 2003]. The high N/P ratio in the negative relationship indicates the influence of CDW (Fig. 3.4c). The subsurface layer of nitrate-rich water from Changjiang River plumes propagated eastward, but the nutrients were not exhausted due to the insufficient light intensity. Turbid surface water containing the suspended matter limits the light penetration into the subsurface layer and may inhibit the consumption of nutrients [*Isobe and Matsuno*, 2008]. Thus, a distribution with a negative relation between the nitrate and salinity was observed in the study area even though it was far from the Changjiang Estuary. The layer between 20 and 40 m around the nitracline, i.e., around the boundary of the mixing line, which can be used to discriminate between CDW and KSSW, was a mixed layer of high and low N/P ratio water. It can be inferred that this area is a complicated layer that is associated with two major nutrient supplies around the SCM from different sources, even allowing for the interannual variation of CDW expansion.

3.3. Snapshot measurements

3.3.1. Vertical nutrient flux

Water sampling and turbulence measurements were conducted concurrently at 20 stations during the three cruises. Turbulence measurement data obtained at G1 (2010, 2011) and B3 (2010) during the tracing of a satellite-tracked drifting buoy were included in the calculation of the flux, in addition to measurements along the zonal and meridional sections. Nitrate and phosphate gradients, vertical eddy diffusivity, vertical nitrate flux, and phosphate flux averaged within the nitracline at each station are given in Table 3.1.

We divided the observation sites into three groups according to the N/P ratio within the nitracline. The groups LNP and HNP were defined previously and MNP were defined as medium N/P ratio within the nitracline, where the N/P ratio was between 15 and 20. The mean value and 95% confidence interval (CI) in each group were calculated by the bootstrap method. The mean N/P ratio in each group was 12.4 (11.2−13.6), 16.8 (15.7−18.0), 45 (33−61), respectively (hereafter, the mean is written with the 95% CI in parentheses).

The nitrate gradient at the nitracline had ranged from 0.41 (B3, 2010)~2.22 (MD7, 2010) mmol m^{-4} , i.e., within one order of magnitude. However, vertical eddy diffusivity within the nitracline had a large range of 1 (G1, 2010)~72 (MD7, 2009) $\times 10^{-6}$ m^2 s^{-1} and the vertical nitrate flux also had a correspondingly large range of 0.09 (G1, 2010)~3.65 (MD7, 2009) mmolN m^{-2} d^{-1}. The nitrate flux was not definitely proportional to vertical eddy diffusivity, for example, the nitrate flux is not large due to the small vertical nitrate gradient even with large vertical eddy diffusivity exceeding 10^{-5} m^{2}s^{-1} in case of station KD2, 2010, but it was more strongly influenced by vertical diffusion than the nitrate

gradient, when comparing the variation range of both the nitrate gradient and vertical eddy diffusivity.

It was observed that variation in the vertical eddy diffusivity and nitrate flux had a strong effect on the variation of the N/P ratio (Fig. 3.5). Vertical eddy diffusivity and nitrate flux are large for LNP, but small for MNP and HNP. In detailed values shown in Table 3.1, the calculated nitrate flux in this area ranged from 0.09 to 3.65 mmolN $m^{-2} d^{-1}$, and the mean and 95% CI of the flux were 0.84 (0.44−1.35) mmolN $m^{-2} d^{-1}$. For each individual group: the nitrate flux ranged from 0.96 to 3.65 mmolN $m^{-2} d^{-1}$, with a mean of 2.05 (1.36−2.85) mmolN $m^{-2} d^{-1}$ for LNP, 0.09 to 0.77 mmolN $m^{-2} d^{-1}$, with a mean of 0.45 (0.27−0.61) mmolN $m^{-2} d^{-1}$ for MNP, 0.09 to 0.49 mmolN $m^{-2} d^{-1}$, with a mean of 0.22 (0.14−0.33) mmolN $m^{-2} d^{-1}$ for HNP. The calculated nitrate fluxes exceeded 0.96 mmolN $m^{-2} d^{-1}$ for LNP. However, the fluxes for HNP did not exceed 0.49 mmolN $m^{-2} d^{-1}$ and the mean flux was about one-nineth of that for LNP.

Nitrate-based flux is a major nutrient source for new production around the SCM aside from being influenced by CDW. Assuming the validity of the Redfield ratio (C:N ~ 6.6) for phytoplankton and carbon atomic mass, an average flux of 0.84 (0.44−1.35) mmolN $m^{-2} d^{-1}$ would support a new production of 67 mgC $m^{-2} d^{-1}$. Although the turbulent nitrate flux has a locally large variation, this mean flux is the largest flux so far reported in the ECS when compared to other studies with direct measurements of turbulence [*Liu et al.*, 2013; *Shiozaki et al.*, 2011], and the new production was similar to that reported at the shelf region of the southern ECS using the nitrogen assimilation method [*Chen et al.*, 1999], even though it would include other nitrogen sources from horizontal advection and atmospheric input.

At the sites where the N/P ratio was low at the nitracline, the average flux of 2.05 (1.36−2.85) mmolN $m^{-2} d^{-1}$ was considerable, but not as large as the largest flux published to date, which was estimated at the continental slope of the upwelling region [*Schafstall et al.*, 2010]. Comparing the new production estimated by the nitrate flux with a few reported observations [*Gong et al.*, 2003; *Liu et al.*, 2013; *Shiozaki et al.*, 2011] and model results [*Liu et al.*, 2010], the value presented here was large, despite being far from the estuary. In order to quantify the proportion of new production generated by the turbulent nitrate flux, we estimated primary production using the data in conjunction with hydrographic and biological measurements in our study area, as described in the following section.

3.3.2. Primary production

The IPP had a wide range of 339~1606 mgC $m^{-2} d^{-1}$ and was similar range with other reported summer IPP in the northern ECS [*Chen et al.*, 1999, *Yoon et al.*, 2012, *Gong et al.*, 2003, *Kwak et al.*, 2013]. In the estimation of IPP and IPPS, there may be an uncertainty in the IPP at MD7 (2009) and CLON7 (2009) stations due to the unknown attenuation coefficient. The attenuation coefficients for MD7 and CLON7 (2009) were substituted with those of nearby stations due to the low PAR intensity.

Phosphate is a limiting factor in nitrate-rich estuaries, while nitrate is more important in the offshore region nearside of the Kuroshio. Therefore, the turbulent nutrient flux contributing to the IPPS is shown as the ratio of the nitrate and phosphate fluxes divided by IPPS, in which the N/P ratio is low (medium) and high (Table 3.2), respectively. The mean ratios of primary production estimated by the nutrient flux to IPPS were 0.99 (0.37−1.61) for LNP, 0.31 (0.05−0.67) for MNP, and 0.03 (0.02−0.05) for HNP. Although the ratio has a large variation even within the LNP and MNP group, mean ratio was

31

generally large for the LNP compared with the HNP and MNP (Fig. 3.6). The ratio occasionally exceeded 1 (MD7, 2009, and CK6, MD4, and G1, 2011), namely when the turbulent nutrient flux surpassed the IPPS, partly due to the rough conversion of primary production from the transient nutrient flux. Although instantaneous turbulence measurements did not clearly indicate a representative (or mean) value during a day due to the small number of samples, there is likely to be a considerable level of nutrients supplied to the SCM by the turbulent nutrient flux for LNP.

To sum up the results of snapshot measurements, the estimated vertical nutrient flux had a strong tendency according to the N/P ratio. The difference of mean vertical eddy diffusivity and vertical nutrient flux between LNP and HNP (MNP) was significant. While, in the estimation of primary production, even though IPPS has a large variation of 28~1089 mgC m^{-2} d^{-1}, ensemble mean of IPPS for each group of N/P ratio had a small variation. Accordingly, the ratio of vertical nutrient flux to IPPS had a significant difference between LNP and HNP (MNP). Consequently, the magnitudes of the vertical eddy diffusivity, nutrient flux caused by vertical mixing, and consequent contribution to IPPS were large for LNP, whereas small for HNP and MNP (Fig. 3.7). This indicates that large nutrient flux by vertical mixing from the lower layer lowers the N/P ratio within the nitracline and contributes to the primary production around the SCM.

3.4. Time series measurements

As previously stated, the vertical nutrient fluxes during the snapshot measurements sometimes exceeded the IPPS (Fig. 3.6). This might be misleading of no regenerated primary production in some LNP stations. However, we do not think there is no regenerated PP in those stations because it is exaggerated daily flux attributed from instant snapshot

measurement of Kz when it was much larger than daily mean. If it is possible to estimate

the vertical nutrient flux and IPPS during the time series measurements, it could make up

the inconvenient problem resulted from this large variability of vertical nutrient flux.

The estimation of vertical nutrient flux during times series measurement more than

24 hours can be expected to yield more reasonable value, yielding ensemble mean flux

through the time series rather than a snapshot flux multiplied by 86400 as daily mean,

therefore, enhances the reliability of the concept which holds the large contribution of

vertical nutrient flux to IPPS for LNP argued from the snapshot measurements.

3.4.1. Filling up the nutrient data

In this section, to make up for the uncertainty of snapshot measurements, we

examine the time series of nutrient flux. We obtained time series of microstructure with

repeated cast of TurboMAP every hour (2010 and 2011) or every two hours (2009) for a

few days. However, caused by limitation of working on board, CTD and water sampling

was limited (Table 3.3), particularly at night time, resulting in small number of nutrient

data during the time series. To compensate for the limitations of nutrient measurements,

we tried to estimate the profile of nutrient concentration from temperature.

The nitrate concentration is sometimes correlated with the temperature below the

nitracline in mid-shelf waters as suggested by *Omand et al.*, [2012]. *Liu et al.* [1990] more

credibly showed subsurface water in the Kuroshio linearly increasing nitrate and phosphate

concentrations with decreasing temperature. Considering that the Kuroshio comes into

contact with the shelf water of the northern ECS [*Matsuno et al.*, 2009], this linear

relationship would be helpful to unveil the nutrient concentrations using the temperature

profile. During the limited observations made on board the vessel, we found a linear relationship between the nitrate/phosphate concentration and temperature during each cruise, as shown in Fig. 3.8. The relationship between the nitrate/phosphate concentration and temperature was roughly linear within the nitracline for the data obtained during each period (Table 3.4) The relationship must have large variations in time and space, therefore we used the linear relationship between temperature and nitrate/phosphate concentrations case by case in each period. The regression was conducted individually for two periods in each year due to the changing of sites during the measurements. To compensate for the small number of nutrient samples due to the limited observations, linear regressions with variance were estimated using the bootstrap method.

3.4.2. Vertical nutrient flux

Vertical profiles of nutrient concentrations within the nitracline were reproduced every hour from temperature measurements using the linear regression between the temperature and nitrate/phosphate concentration. Hourly mean vertical nutrient fluxes were investigated during the time series (Fig. 3.9). The vertical nitrate and phosphate fluxes are calculated for LNP and HNP, respectively, to counteract the nutrient limitation. The N/P ratios during each period are determined from a few water samplings made during time series measurements. The vertical nutrient flux had large variation between $O(10^{-3})$ and $O(10^0)$ mmolNm^{-2}h^{-1} during the observation period. Large flux events exceeding $O(10^{-1})$ mmolNm^{-2}h^{-1}, for example, Jul. 19 04:00 and Jul. 20 04:00, 2010 and Jul. 18 00:00 and 22:00, 2011, frequently found during LNP more than HNP is thought to enlarge the vertical nutrient flux and lower the N/P ratio.

3.4.3. Primary production

Hourly IPPS was estimated using the method described in the previous section. Unknown photosynthetic parameters were adapted from the nearest station. Hourly PP-NF was also estimated to compare the IPPS. We finally calculated the integration of the nutrient flux and IPPS during a day. Ensemble mean with variance during each period of time series measurements, is shown in Table 3.5. The averaged N/P ratio within the nitracline was also calculated during each period. Definitely the nutrient flux for LNP is larger than for HNP to the extent of an order of magnitude, while just two or three samples for each group. The mean flux for LNP is over three times greater than for HNP. Large fluxes for LNP have consistency with results of snapshot measurements. The contribution of the flux to primary production for MNP was calculated from both PP-NF and PP-PF. An estimation of the contribution of flux during period 1 of 2009 was impossible because chlorophyll a data was not available due to a malfunction of the fluorescence sensor. On the other hand, in the case of period 2 of 2009, the contribution of the nutrient flux was likely to be overestimated due to the estimations being made only during a third of the day in essence (10 p.m. July 22−10 a.m. July 23), rather than over a full day. The value 0.11 should be corrected to less than half under the assumption of IPPS during the full day.

Estimated values of the contribution indicated a relatively large contribution of the nutrient flux to new production by vertical mixing for LNP compared to HNP. If we considered the directly measured f-ratio of 0.25-0.42 in summer except for upwelling region, as suggested by *Chen et al.* [2001], the vertical nitrate flux is considerably responsible for the new supply of nutrients, especially in the two periods of LNP, 2011 when the deep SCM is formed.

PP-NF, i.e., the new production of nitrate supply caused by vertical mixing, was more than the IPPS (almost zero) during the nighttime and less than the IPPS during the daytime. Because the nutrient supplied by upward fluxes may have exceeded the uptake capacity of phytoplankton, excess nutrients supplied during the nighttime may be utilized in the daytime as reported by *Sharples et al.* [2007].

3.4.4. Vertical chlorophyll flux

Diffusion is the net movement of molecules or atoms from a region of high concentration to a region of low concentration. Therefore, it is worth to consider the movement of chlorophyll as well as nutrients by diffusion. We tried to estimate a reduction in primary production by chlorophyll erosion within the nitracline.

The chlorophyll flux was calculated by multiplying vertical eddy diffusivity with the vertical gradient of chlorophyll a concentration using Fickian diffusion theory, $F = -Kz\, \partial C/\partial z$, same as the calculation of vertical nutrient flux. The chlorophyll flux was calculated within the nitracline but adjusted upper boundary to the depth of SCM. The chlorophyll flux has a negative value, a downward flux, and exports from the upper layer to the lower layer within this interval.

To convert chlorophyll flux into a primary production, we assume a constant C:chlorophyll a ratio of 40 for SCM phytoplankton [*Holligan et al.*, 1984, *Williams et al.*, 2013]. Primary productions converted from the calculated chlorophyll fluxes were showed in Table 3.6 with nutrient fluxes for comparison. The percentages of chlorophyll flux to nutrient flux were 18, 14, 20, 11, 7 for period 2 of 2009, period 1 and 2 of 2010, and period 1 and 2 of 2011, respectively. The mean percentage was 13, that is, the nutrient flux was

seven times more than the chlorophyll flux. Despite some uncertainty about the C:chlorophyll a ratio, the chlorophyll flux derived from the vertical mixing was small compared to the nutrient flux.

Tables

Table 3.1 Calculated nitrate gradient ($\partial NO_3^-/\partial z$), vertical eddy diffusivity (K_z), vertical nitrate flux (*NF*), vertical phosphate flux (*PF*), and mean N/P ratio within the nitracline. The numbers in parentheses denote the 95% confidence interval

Station	$\partial NO_3^-/\partial z$ (mmol m^{-4})	$\partial PO_4^-/\partial z$ (mmol m^{-4})	K_z ($\times 10^{-6}$ m^2 s^{-1})	*NF* (mmolN m^{-2} d^{-1})	*PF* (mmolP m^{-2} d^{-1})	N/P ratio
MD7, '09	0.59	0.021	72	3.65	0.127	12.9
CLON7, '09	0.83	0.006	35	2.48	0.017	14.7
CLON5, '09	0.66	0.009	17	0.96	0.013	13.2
MD5, '10	0.89	0.063	24	1.82	0.130	10.9
CK6, '11	0.80	0.054	23	1.61	0.109	10.0
MD4, '11	0.95	0.055	22	1.80	0.104	12.8
mean	0.79(0.69-0.88)	0.035(0.018-0.055)	32(21-50)	2.05(1.36-2.85)	0.083(0.035-0.121)	12.4(11.2-13.6)
MD1, '09	1.08	0.036	8	0.77	0.025	15.7
MD7, '10	2.22	0.124	3	0.49	0.027	16.7
CLON4, '10	0.63	0.017	8	0.45	0.013	18.7
KD2, '10	0.51	0.020	13	0.55	0.021	18.5
G1, '10	0.86	0.046	1	0.09	0.005	15.5
G1, '11	0.52	0.047	8	0.36	0.044	15.8
mean	0.97(0.57-1.54)	0.048(0.026-0.093)	6.8(3.3-10.5)	0.45(0.27-0.61)	0.023(0.011-0.034)	16.8(15.7-18.0)
MD5, '09	1.09	0.029	4	0.34	0.009	93
MD3, '09	0.63	0.003	9	0.49	0.003	51
CLON3, '09	0.64	0.024	2	0.13	0.005	35
CLON1, '09	0.52	0.009	3	0.15	0.003	46
MD3, '10	1.04	0.063	2	0.16	0.010	34
MD1, '10	0.51	0.023	2	0.09	0.004	34
B3, '10	0.41	0.029	5	0.17	0.012	35
MD3, '11	0.53	0.024	4	0.19	0.009	29
mean	0.67(0.52-0.85)	0.026(0.013-0.039)	3.9(2.4-5.6)	0.22(0.14-0.33)	0.007(0.004-0.010)	45(33-61)

Table 3.2

Depth of SCM, integrated primary production within the euphotic zone (IPP), primary production converted from the nitrate flux (PP-NF) in case for LNP and MNP, primary production converted from the phosphate flux (PP-PF) in case for HNP, a ratio of the nutrient flux to integrated primary production within the vicinity of SCM (IPPS), and the N/P ratio within the nitracline. The numbers in parentheses denote the 95% confidence interval

Station	Depth of SCM (m)	PP-NF or PP-PF (mgC m^{-2} d^{-1})	IPP (mgC m^{-2} d^{-1})	IPPS (mgC m^{-2} d^{-1})	PP-NF/IPPS(LNP) PP-PF/IPPS(HNP)	N/P ratio
MD7, '09	18	289	*1123	*189	1.70	12.9
CLON7, '09	7	196	*1308	*914	0.24	14.7
CLON5, '09	12	76	1482	735	0.11	13.2
MD5, '10	23	144	1096	252	0.64	10.9
CK6, '11	29	128	339	64	2.23	10.0
MD4, '11	29	143	904	154	1.03	12.8
mean	20(12-26)	163(113-234)	1042(721-1329)	385(136-664)	0.99(0.37-1.61)	12.4(11.2-13.6)
MD1, '09	11	61	1141	1089	0.06	15.7
MD7, '10	17	39	816	126	0.34	16.7
CLON4, '10	7	36	993	619	0.06	18.7
KD2, '10	23	44	549	206	0.24	18.5
G1, '10	15	7	1188	372	0.02	15.5
G1, '11	27	29	413	28	1.12	15.8
mean	17(11-23)	36(20-50)	850(632-1051)	407(148-735)	0.31(0.05-0.67)	16.8(15.7-18.0)
MD5, '09	12	11	701	329	0.04	93
MD3, '09	16	4	715	376	0.01	51
CLON3, '09	18	6	939	324	0.02	35
CLON1, '09	19	4	506	59	0.07	46
MD3, '10	23	13	736	435	0.03	34
MD1, '10	8	5	1606	986	0.01	34
B3, '10	9	15	786	351	0.05	35
MD3, '11	24	11	1070	612	0.02	29
mean	16(11-20)	9(6-11)	882(684-1173)	434(272-662)	0.03(0.02-0.05)	45(33-61)

Table 3.3 Summary of observation time during time series measurement

	Period or measurement time	
	Turbulence	Nutrient concentrations
2009	16:00 19 - 14:00 21 July 6:00 22 - 8:00 23 July (every two hours)	12:00 20 10:00 21 14:00 22 12:00 23 July
2010	1:00 19 - 18:00 21 July 13:00 22 - 17:00 23 July (every hour)	12:00 19 12:00 20 12:00 22 6:00 23 8:00 23 12:00 23 July
2011	22:00 16 - 14:00 19 July 9:00 20 - 16:00 21 July (every hour)	13:00 17 12:00 18 12:00 21 13:00 21 July

Table 3.4

Linear regression between the temperature and nitrate/phosphate concentration during the observation period

	Period 1		Period 2	
	Regression of NO_3 ($mmolm^{-3}$) / Regression of PO_4 ($mmolm^{-3}$)	Period	Regression of NO_3 ($mmolm^{-3}$) / Regression of PO_4 ($mmolm^{-3}$)	Period
2009	$\begin{cases} 25.995 - 1.053T & (T < 24.7°C) \\ 0 & (T > 24.7°C) \end{cases}$ R = 0.95 / $\begin{cases} 0.994 - 0.045T & (T < 22.1°C) \\ 0 & (T > 22.1°C) \end{cases}$ R = 0.73	16:00 19 Jul. - 14:00 21 Jul.	$\begin{cases} 35.819 - 1.640T & (T < 21.8°C) \\ 0 & (T > 21.8°C) \end{cases}$ R = 0.97 / $\begin{cases} 1.058 - 0.0481T & (T < 22°C) \\ 0 & (T > 22°C) \end{cases}$ R = 0.65	6:00 22 Jul. - 8:00 23 Jul
2010	$\begin{cases} 89.019 - 6.316T & (T < 14.1°C) \\ 0 & (T > 14.1°C) \end{cases}$ R = 0.74 / $\begin{cases} 6.627 - 0.465T & (T < 14.3°C) \\ 0 & (T > 14.3°C) \end{cases}$ R = 0.82	1:00 19 Jul. - 18:00 21 Jul.	$\begin{cases} 81.167 - 5.851T & (T < 13.9°C) \\ 0 & (T > 13.9°C) \end{cases}$ R = 0.88 / $\begin{cases} 3.894 - 0.272T & (T < 14.3°C) \\ 0 & (T > 14.3°C) \end{cases}$ R = 0.78	13:00 22 Jul. - 17:00 23 Jul.
2011	$\begin{cases} 53.291 - 3.843T & (T < 13.9°C) \\ 0 & (T > 13.9°C) \end{cases}$ R = 0.95 / $\begin{cases} 2.784 - 0.203T & (T < 13.7°C) \\ 0 & (T > 13.7°C) \end{cases}$ R = 0.93	22:00 16 Jul. - 14:00 19 Jul.	$\begin{cases} 69.045 - 4.910T & (T < 14.1°C) \\ 0 & (T > 14.1°C) \end{cases}$ R = 0.98 / $\begin{cases} 7.022 - 0.523T & (T < 13.4°C) \\ 0 & (T > 13.4°C) \end{cases}$ R = 0.99	9:00 20 Jul. - 16:00 21 Jul.

Table 3.5

Estimated PP-NF and PP-NF/IPPS in case for LNP, PP-PF and PP-PF/IPPS in case for HNP, both PP-NF and PP-PF, PP-NF/IPPS and PP-PF/IPPS in case for MNP, and the corresponding N/P ratio during the observation period in time series measurements

	Period 1			Period 2		
	PP-NF or PP-PF ($mgC\ m^{-2}\ d^{-1}$)	**PP-NF/IPPS** or PP-PF/IPPS	N/P ratio	**PP-NF** or PP-PF ($mgC\ m^{-2}\ d^{-1}$)	**PP-NF/IPPS** or PP-PF/IPPS	N/P ratio
2009	24	-	HNP (33.3)	38	[†]0.11	HNP (29.0)
2010	**73 (65-82)**	**0.26 (0.21-0.31)**	LNP (11.4)	**60 (56-66)** 49 (46-53)	**0.28 (0.20-0.36)** 0.23 (0.16-0.32)	MNP (16.0)
2011	**170 (160-178)**	**0.48 (0.44-0.52)**	LNP (13.9)	**67 (58-75)**	**0.18 (0.15-0.20)**	LNP (13.9)

[†] See text about the relatively high value as HNP.

Table 3.6

Estimated vertical nutrient flux (**PP-NF** or PP-PF) and chlorophyll flux (PP-CF) during the observation period in time series measurements. Both nutrient flux and chlorophyll flux are converted to primary production for comparison between them. PP-NF in case for LNP, PP-PF in case for HNP is in same use shown in Table 3.4

	Period 1		Period 2	
	PP-NF or PP-PF $(mgC\ m^{-2}\ d^{-1})$	PP-CF $(mgC\ m^{-2}\ d^{-1})$	**PP-NF** or PP-PF $(mgC\ m^{-2}\ d^{-1})$	PP-CF $(mgC\ m^{-2}\ d^{-1})$
2009	24	-	38	7 (2-16)
2010	**73 (65-82)**	10 (7-13)	**60 (56-66)** 49 (46-53)	12 (11-13)
2011	**170 (160-178)**	18 (17-19)	**67 (58-75)**	5 (4-6)

Figures
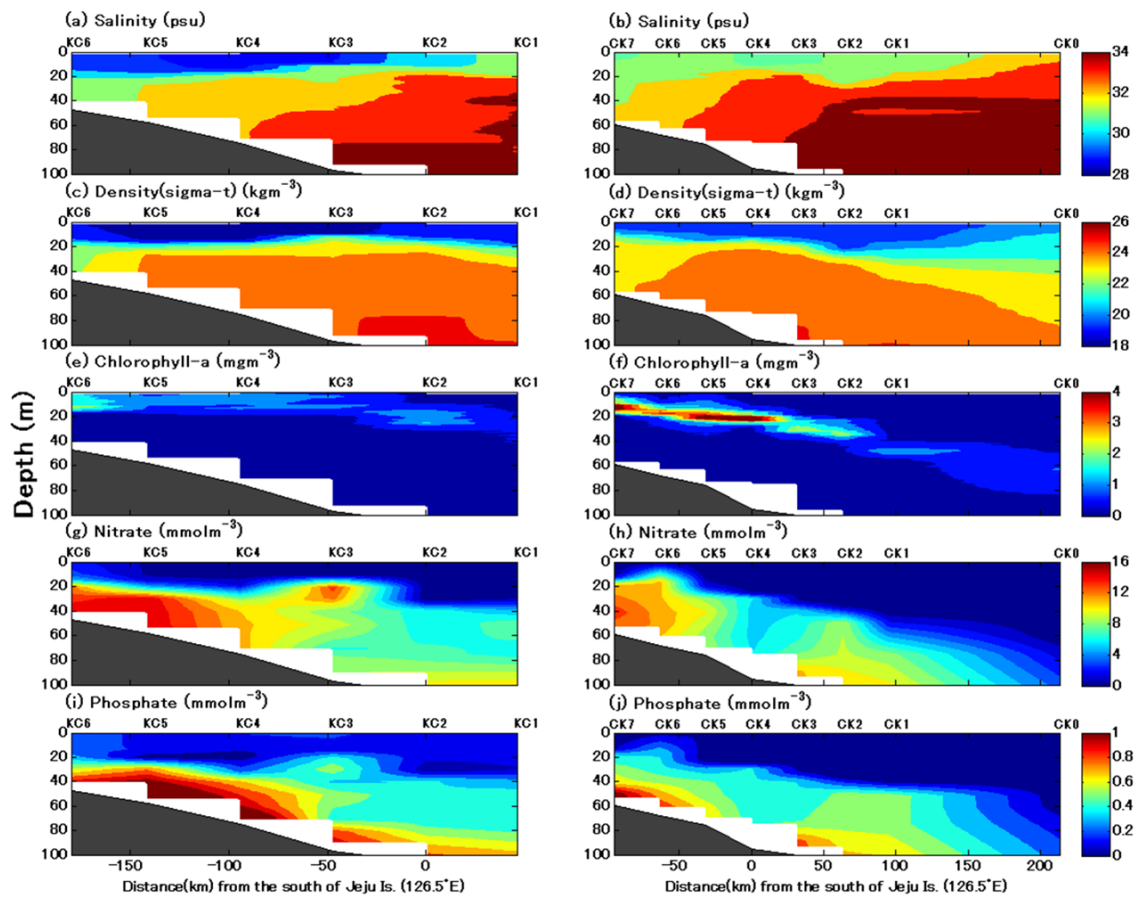
Fig. 3.1 Vertical structures of salinity (a, b), density (c, d), and fluorescence (e, f) calibrated with the chlorophyll a, nitrate (g, h), and phosphate concentrations (i, j) along CDW expansion in two horizontal sections, KC (left panel) and CK (right panel) transects, 2009. The colored areas representing the levels of nitrate and phosphate concentrations are fitted to match the Redfield ratio (N:P = 16:1). The horizontal axis is expressed as the distance from the south of Cheju Island on the same latitude.
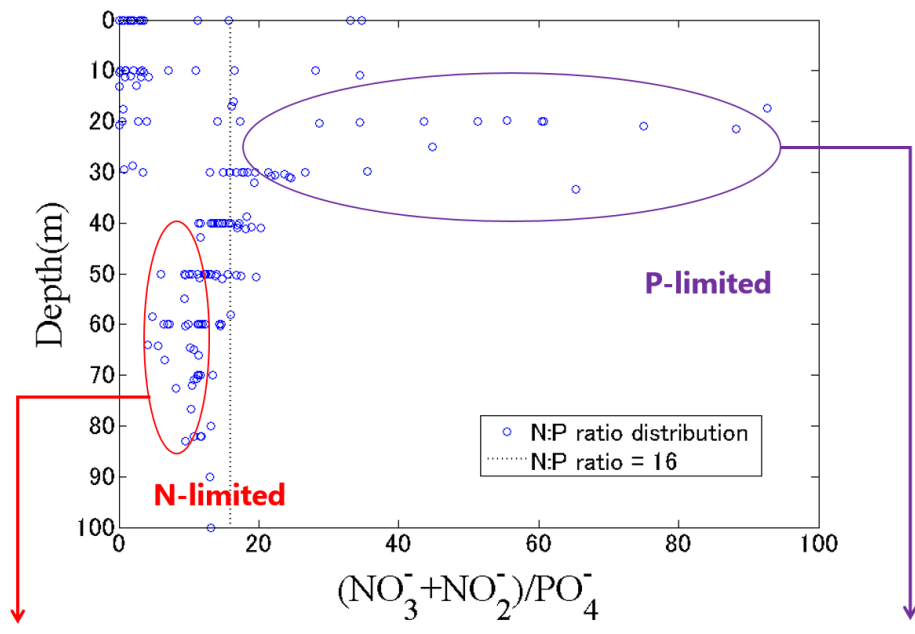
44

**Fig. 3.2** Vertical distribution of N/P ratio from all water samples.
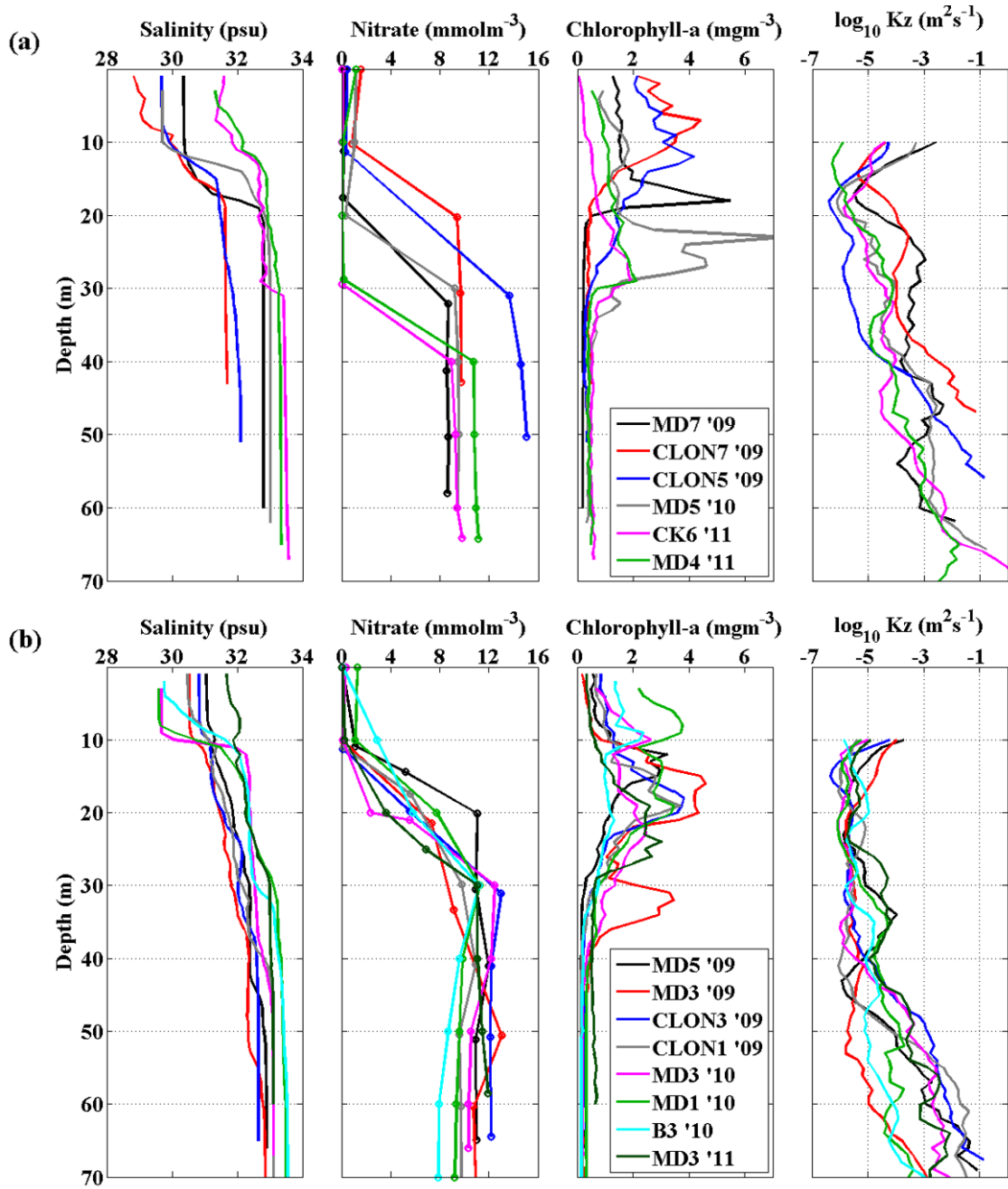
Fig. 3.3 Vertical profiles of salinity, nitrate, chlorophyll a, and vertical eddy diffusivity (*Kz*) at stations where turbulence measurements were made when the N/P ratio was low (a) and high (b) within the nitracline. Vertical eddy diffusivity is presented on a log scale.
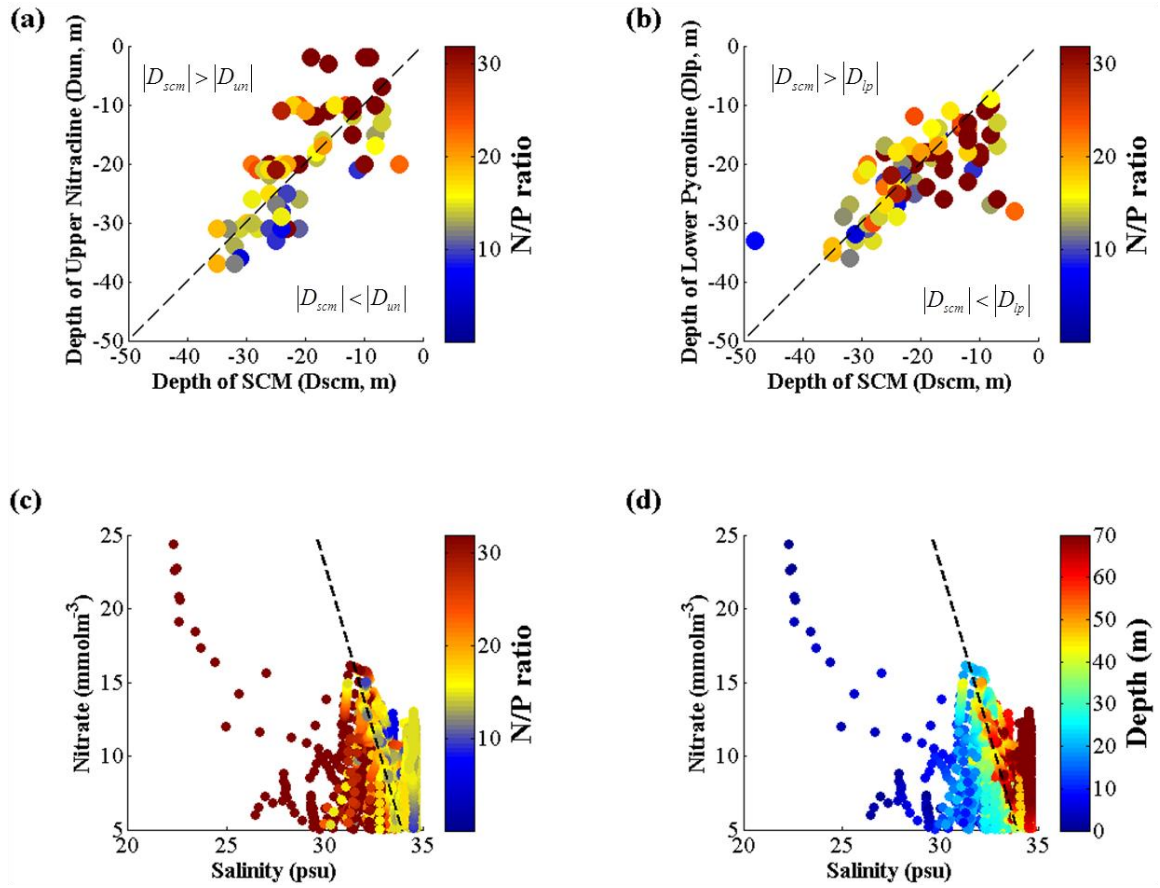
Fig. 3.4 Relationship between the depth of the subsurface chlorophyll maximum (SCM) and the upper boundary of the nitracline (a), and the lower boundary of the pycnocline (b) combined for all stations. The color indicates the N/P ratio within the nitracline at each station. The relationship between the nitrate concentration and salinity collected from all profiles in accordance with the N/P ratio (c) and sampling depth (d). The dashed line is the hypothetical mixing line for two end members ($\partial NO_3^-/\partial S = -4.6$).
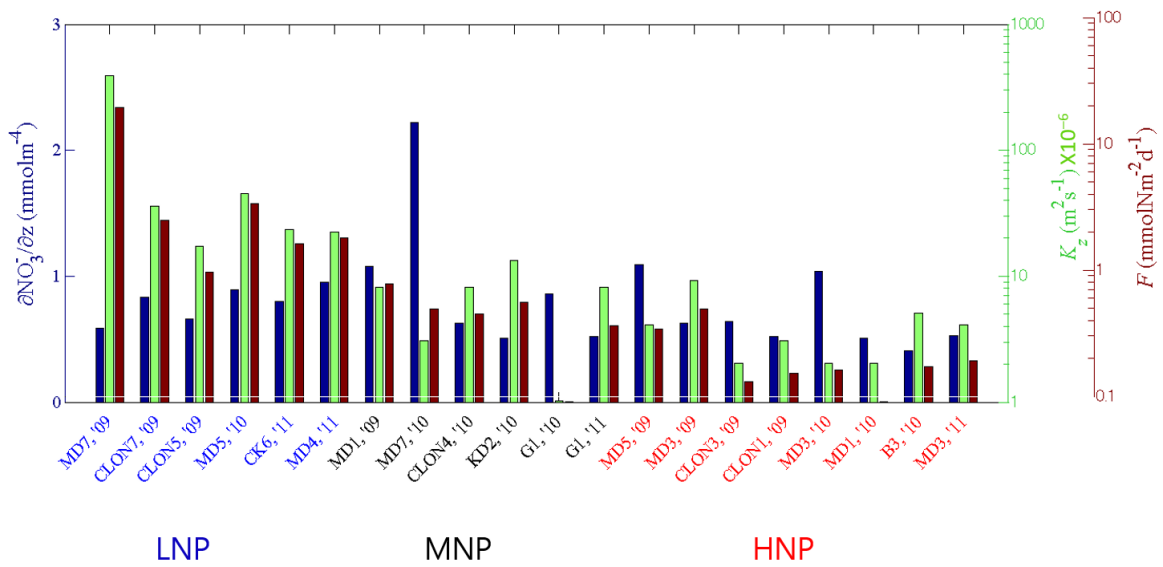
Fig. 3.5 Calculated nitrate gradient (blue), vertical eddy diffusivity (Kz, green) and nitrate

flux (F, red) for individual station.
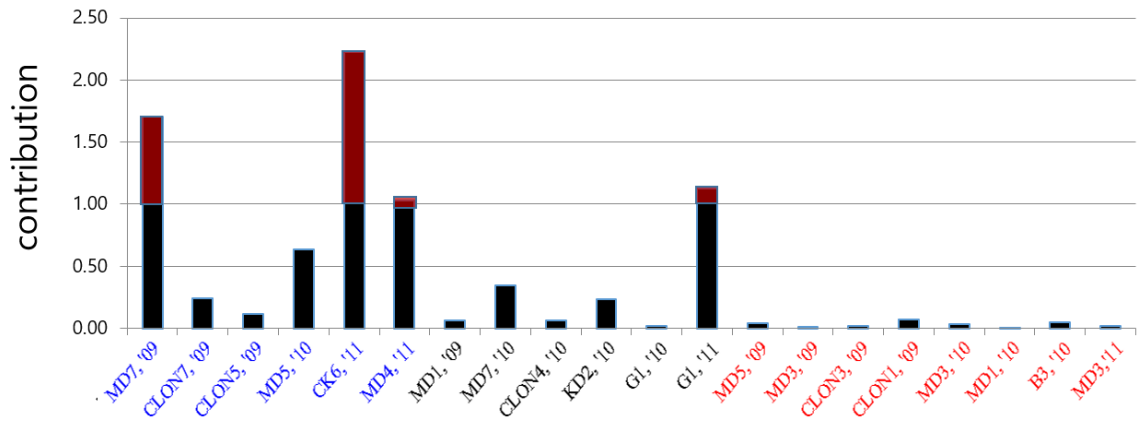
Fig. 3.6 Contribution of vertical nutrient flux to IPPS for each station. Each station is arranged from low to high according the N/P ratio.
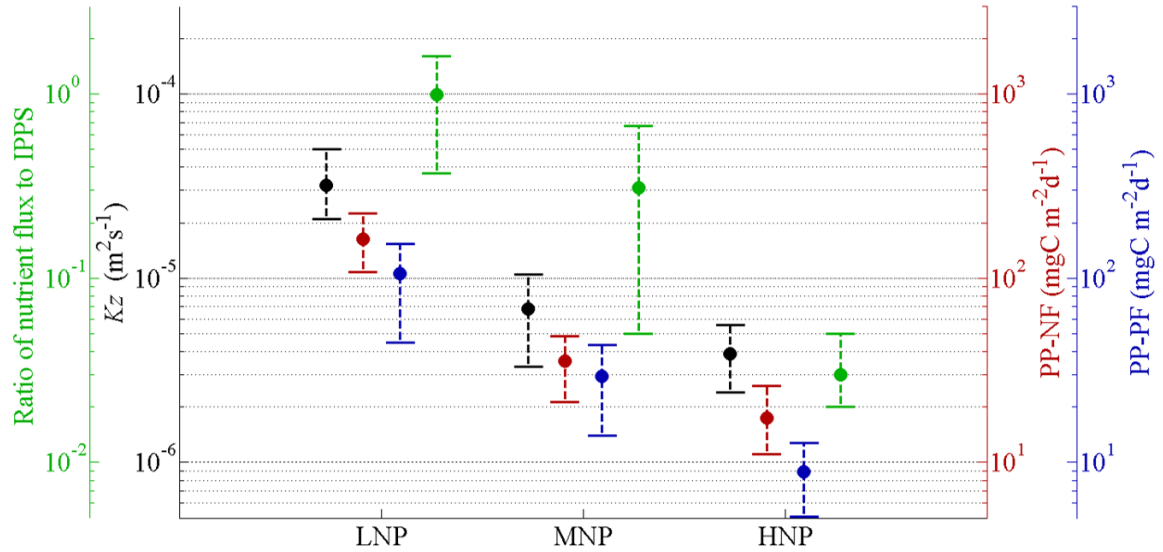
Fig. 3.7 Mean (circle) and 95% confidence interval (dotted line with two solid lines) of vertical eddy diffusivity (*Kz*) (black), primary production converted from the nitrate flux (red), primary production converted from the phosphate flux (blue) and the ratio of the nutrient flux to IPPS (green) for LNP, MNP, and HNP. The 95% confidence intervals for vertical eddy diffusivity and fluxes were calculated by the bootstrap method.
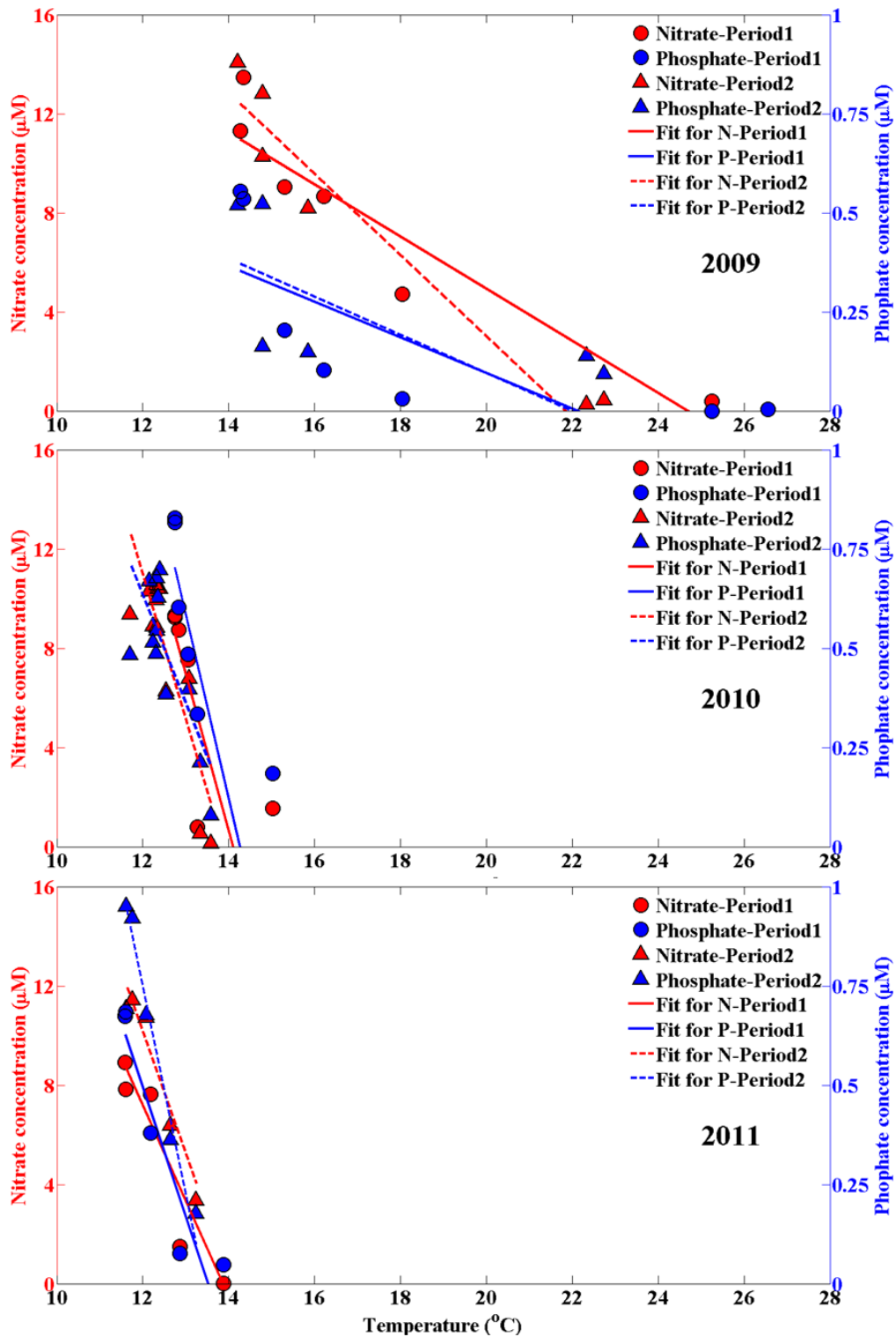
Fig. 3.8 Relationship between the temperature and nitrate/phosphate concentrations during each period. A linear regression was fitted only within the nitracline.
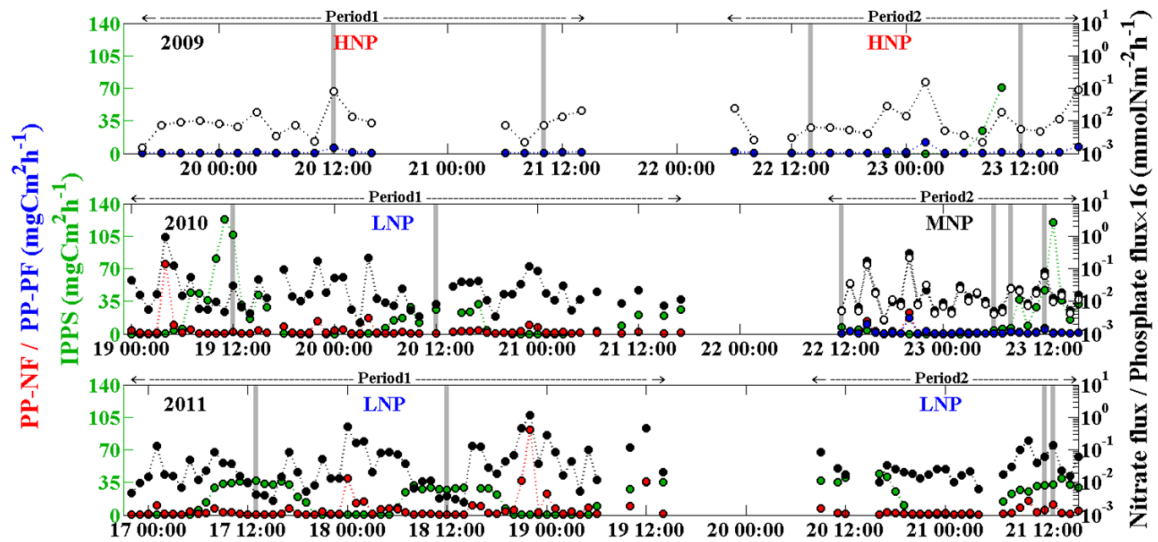
Fig. 3.9 Time series of vertical nitrate flux (black circle) and phosphate flux (open circle), IPPS (green circle), and primary production converted from the vertical nitrate flux (red circle) and phosphate flux (blue circle). The vertical nitrate flux and converted primary production were presented only for LNP, the vertical phosphate flux and converted primary production were presented only for HNP, and both nitrate and phosphate fluxes and converted primary productions were presented for MNP. The green circles are plotted first, and then black, open, red, and blue circles are overlapped in turn for period 2 of 2010. The phosphate flux was multiplied by 16 to compare the magnitude of nitrate flux intuitionally. Thick gray lines indicate the time when water samplings were made during the time series measurements of turbulence.

4. Discussion

4.1. Observed turbulence driving considerable nutrient supply into the SCM

Vertical profiles of ε, the squared buoyancy frequency N^2, and vertical eddy diffusivity K_z of snapshot measurements are shown in Fig. 4.1-4.5. The magnitude of ε varied vertically between $O(10^{-10})$ and $O(10^{-6})$ Wkg^{-1}, while a strong turbulent dissipation was found frequently at subsurface and above the bottom, having a magnitude sometimes exceeding $O(10^{-7})$ Wkg^{-1}. Coincidently, the K_z showed similar vertical distribution pattern to ε. Large values of K_z were found frequently around the subsurface layer, such as around 11 m at station CLON7, 2009 and around 12 m at station CLON5, 2009, around 12 m at station MD5, 2010, around 14 m at G1, 2011 and 20−30 m above the bottom of almost stations with the magnitude exceeding 10^{-4} m^2s^{-1}.

Meanwhile, focused on the turbulence within the nitracline, the magnitude of K_z varied between $O(10^{-5})$ and $O(10^{-3})$ Wkg^{-1} at LNP stations (MD7, CLON7, CLON5, 2009, and MD5, 2010, and CK6, MD4, 2011), larger than those of other stations with the magnitude between $O(10^{-6})$ and $O(10^{-5})$ Wkg^{-1} consistent with the mean values as shown in Table 3.1. This results explain that large nutrient flux from the lower layer enhances the supply of phosphate rich water and lowers the N/P ratio.

Based upon the results of turbulence measurements, two possibilities are considerable resulting in large K_z and vertical diffusion flux. One of large turbulence occurred at subsurface layer might be attributed to the internal waves frequently observed in the shelf region of the East China Sea. *Lee et al.,* [2006] showed that internal wave-induced mixing and tidal friction could be responsible for the dissipation enhancement at

these depths. Our measurement also showed the large ε at subsurface, such as station CLON7 and CLON5, 2009. Large ε is a clue for large Kz and vertical diffusion flux and this is not attributed to low value of N^2 unless the water is occasionally mixed within the pycnocline.

The other is overlapping the nitracline with the upper bottom boundary layer which is vigorous turbulence layer induced by bottom stress due to tidal currents as reported by *Matsuno et al.*, [2005, 2009], when a relatively deep SCM is formed closer to the bottom boundary layer. Those locations might be related with the interannual variation of temperature structure which is one of main components for the primary production as well as light and nutrients.

4.2. *Physical processes providing a nutrient supply for new production*

We attempted to estimate the nutrient supply resulting in primary production at the continental shelf of the ECS. Two major sources act on the nutrient supply through different processes. One is CDW, by horizontal advection, and the other is KSSW or subsurface water on the shelf by vertical mixing and advection in physical processes. Precipitation, and biochemical processes such as nitrogen fixation and nitrification within the euphotic zone, could also be sources of nutrient supply leading to new production. In this study, we focused on the turbulent nutrient flux supplied into the SCM because vertical mixing could be a key process providing a nutrient supply, if there is no horizontal input of nutrients from CDW.

Significant difference of the contribution of the nutrient flux to IPPS between HNP and LNP pointed out that nutrients have been sufficiently supplied by vertical mixing

regardless of horizontal advection considering the N/P ratio by means of observation result which reflects the present condition. The ratios of nutrient flux to IPPS for LNP indicate a sufficient contribution of nutrient supply by vertical mixing, but most HNP stations had extremely small ratios (Table 3.2). The time series measurements also showed a similar feature (Table 3.4). While, there exists small contribution of flux for a few LNP stations, which forms shallow SCM. There might be other nutrient supplies to satisfy the large IPPS despite large supply of the vertical nutrient flux. The small contribution for HNP and shallow SCM in LNP stations indicate that the horizontal movement of CDW might be considered to have a major role in the nutrient balance.

Meanwhile, upwelling brings not only saline water but also nutrients, resulting in enhanced primary production. *Matsuno et al.* [2006] suggested that the salinity increase during the passage of low pressure measured with the Lagrangian method in CDW could not be explained without significant vertical advection, and showed that vertical mixing was of insufficient magnitude to explain the increase in salinity. The amount of nutrients supplied by vertical advection under calm conditions is uncertain, but sporadic events such as a tropical depression can have a significant effect on nutrient supply from the lower layer. As suggested by *Siswanto et al.* [2008], sporadic events could lead to significant primary production with vertical advection, and could influence primary production in the surface layer, which has been detected by satellite remote sensing. On the other hand, a SCM is commonly found even under calm conditions, during which vertical advection would not play an important role in the salinity change in the surface layer, as suggested by *Matsuno et al.* [2006]. Because the nitracline exists down to 40 m, it is not clear if

55

Ekman transport by surface divergence affects the vertical migration of intermediate water around the nitracline.

4.3. Uncertainties in the estimation of nutrient flux and primary production

Our estimation contained uncertainties in the estimation of nutrient flux and primary production. One of the uncertainties was the measurement of the nitrate gradient for calculating the nitrate diffusion flux. Water sampling was conducted with depth intervals of 10 m, and therefore the nitrate concentrations between the individual sampling depths were unknown. To obtain a more detailed vertical structure, another measurement was made to acquire the fine structure of nitrate and chlorophyll a concentrations. Fig. 4.6 shows the vertical profile of the nitrate concentration, chlorophyll a concentration, vertical eddy diffusivity, and diffusion flux calculated for broad and narrow depth bins from standard and fine CTD measurements and water sampling using the Kz with every meter. A positive nitrate flux indicates an upward flux. The nitrate gradient in narrow depth bins was larger than in broad depth bins at both stations. The fluxes were more precisely estimated from 1.61 to 1.94 mmolN m^{-2} d^{-1} at station CK6, 2011 and from 0.36 to 0.53 mmolN m^{-2} d^{-1} at station G1, 2011. This means that our previous calculation underestimated the fluxes by about 20 % and 47 % at CK6 and G1, 2011, respectively. It is likely that the vertical flux could be larger than that calculated from the measurements, although the nitrate flux calculated with the usual sampling interval was compared with flux calculated using a finer sampling structure at just two stations.

Gross production is usually converted to net production by multiplying by between 0.7 and 0.9 to exclude the respiration of phytoplankton. We selected 0.9 as the value of the

coefficient to evaluate how much the nutrient flux contributes to primary production at least. Nutrient supplies with vertical mixing, advection, and horizontal inputs only contribute to the new production within the subsurface layer, i.e., regeneration by autotrophic phytoplankton is unknown in IPP. In other words, our estimated IPP includes some portion of regenerated primary production besides considerable new supply by vertical mixing and small new supply by other processes for LNP. The f-ratio, the ratio of new production to total production (new production plus regenerated production), must vary between different observation sites despite being not identified in our estimation of new production. Accurate values of the net production rate and f-ratio are important estimating precise new production for comparison with the vertical nutrient flux, but the calculated flux and primary production showed that a significant amount of the nutrient supply is derived from vertical mixing.

The C:chlorophyll a ratio vary with species of phytoplankton and availability of light and nutrients [*Cullen*, 1982]. Thus, the ratio would surely change with the locality and water depth. *Chang et al.*, [2003] estimated the C:chlorophyll a ratio of 67.4 at shelf zone of the ECS, very close to our observation area, but sampled at 5 m. If the phytoplankton above the chlorophyll maximum is light-saturated and possibly nutrient-limited, C:chlorophyll a ratio will be higher near the surface. He also suggested the ratio of 36.1 at 40 m depth. This value is well within the 10-52 range reported for the subsurface chlorophyll maximum [*Furuya*, 1990, *Christian and Karl*, 1994, *Holligan et al.*, 1984]. Considering our calculation layer of 10-30 m for chlorophyll flux, it is appropriate to determine the adopted ratio with 40, but its accuracy needs further verification.
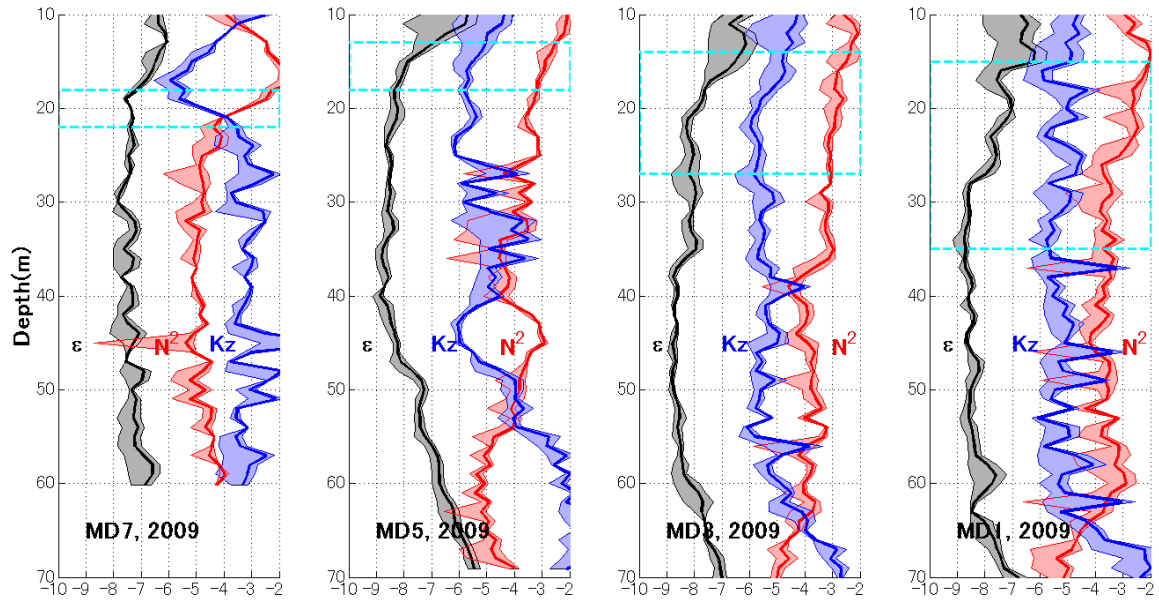
4.4. *Consistency of vertical eddy diffusivity*

In snapshot measurements, the discordance between the turbulence measurement and the estimation of primary production has to be considered before discussing the contribution of the vertical nutrient flux to new production. The turbulence measurement at each station was a snapshot, whereas we estimated primary production with daily integration. It is not certain that a snapshot measurement of turbulence is representative of a full day and it is not known how long the intensity of Kz lasts. Because of the large variability of Kz, it is difficult to estimate the magnitude of daily Kz throughout the period necessary for the daily estimated primary production. Thus, we used a statistical approach to investigate the consistency and range of Kz through successive observations (time series measurements).

What was the difference between the observed Kz and daily estimate? To answer this, we investigated the ratio of the observed Kz and mean Kz within a certain time interval. First, we calculated the mean Kz at a fixed time interval (observed time $\pm$ 2, 4, 6, 8, 10, 12 hrs) as many as possible in whole time series during each year and determined the distribution, median, and 0% and 75 % quantiles of the relative ratio (Fig. 4.7). The median, and the interval between the quartiles, increased with the increasing time interval due to the larger difference between the observed and mean Kz with a larger number of samples. A large variation of Kz could yield more than a 10-fold difference. The 3rd quartile of the ratio indicated that most of variation (75%) was less than 10-fold (or 1/10-fold). Based on the median, the ratios were fixed at under 4-fold (or 1/4-fold) especially for $\pm$ 12 h consistency. Therefore, the observed Kz was significant within a 4-fold variation in the daily estimation. Daily variation of the observed Kz ($<$ 4-fold) is less than the variation of

Kz between LNP and HNP (> 8-fold). This means that the results, vertical nutrient flux is much larger in LNP than HNP, from snapshot measurements should be significant, according to the statistical evaluation with time series measurements.

Figures

Fig. 4.1 Vertical profiles of dissipation rate of turbulent kinetic energy (ε), square of buoyancy frequency (N^2), vertical eddy diffusivity (Kz) in MD transect in 2009. The thick line and shaded area indicates the mean and 95 % confidence interval, respectively. Horizontal axis is presented on a log scale. The cyan rectangle is the layer of nitracline.
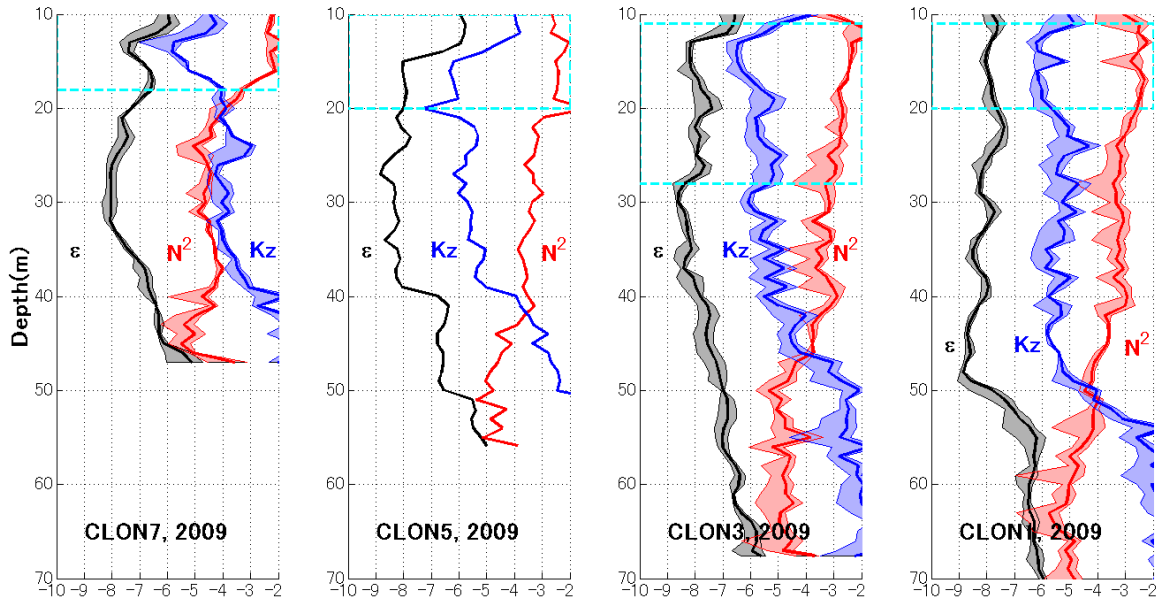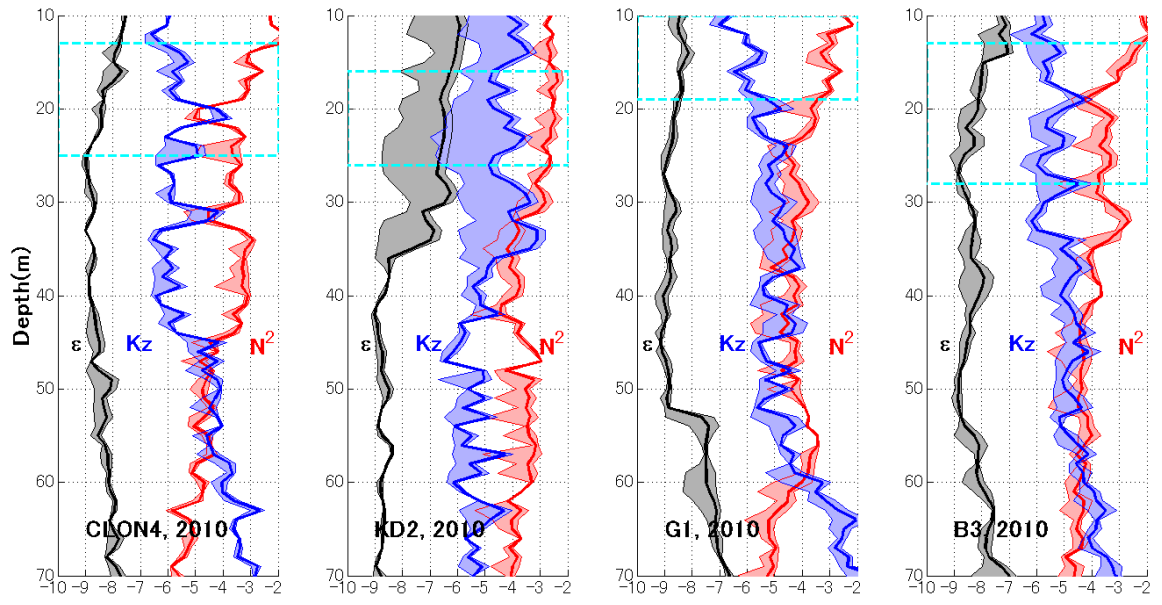
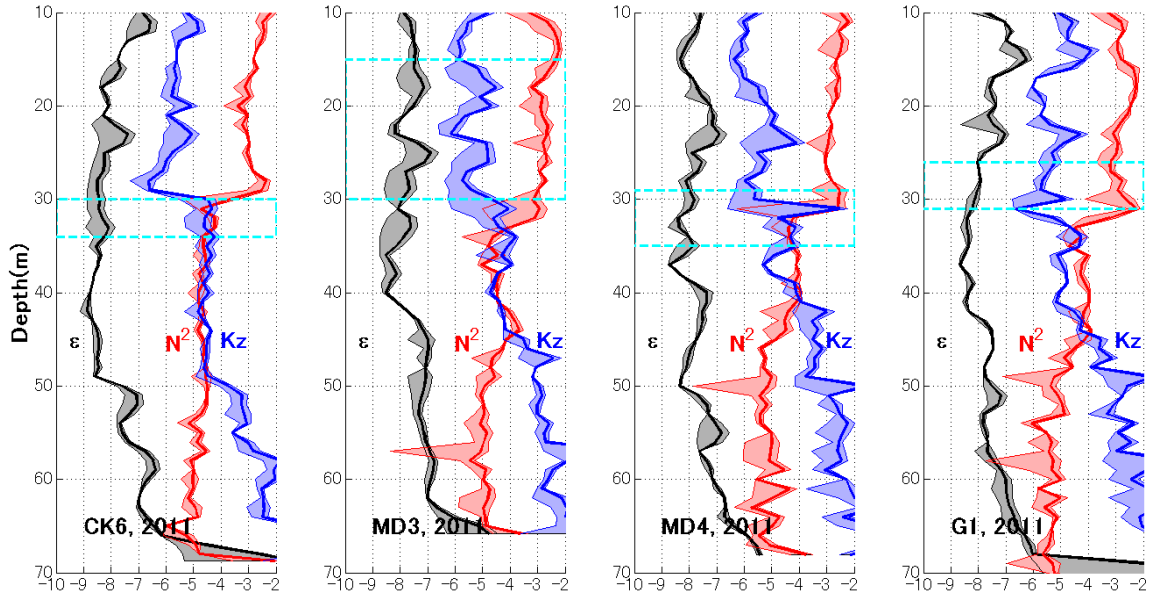**Fig. 4.2** Same as fig. 4.1, but CLON transect in 2009
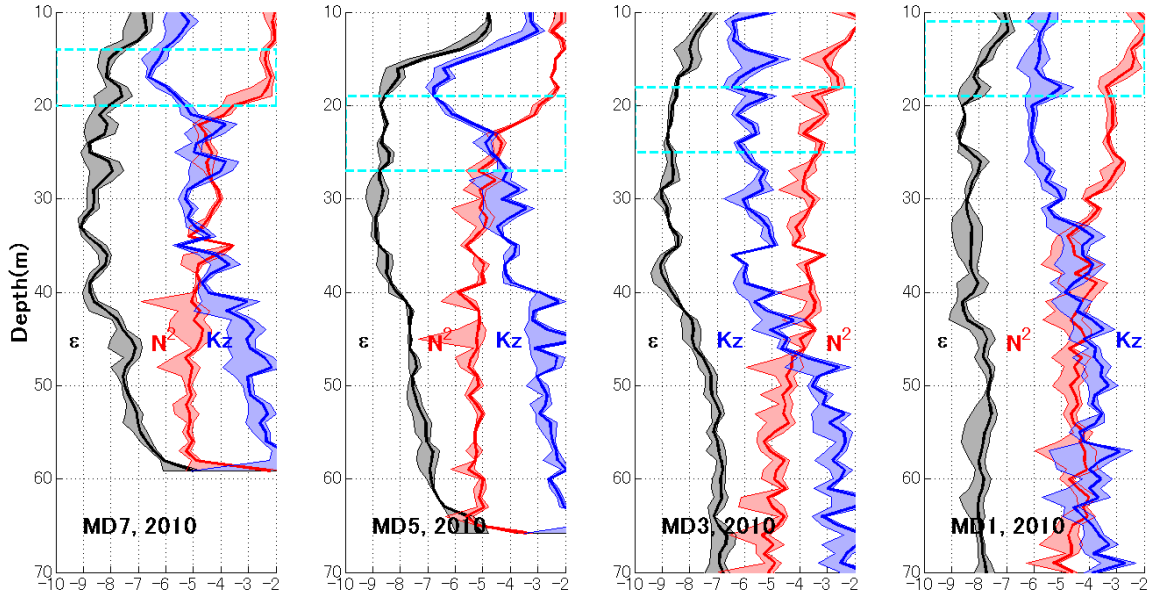
Fig. 4.3 Same as fig. 4.1, but MD transect in 2010.

**Fig. 4.4** Same as fig. 4.1, but other TurboMAP stations in 2010.

Fig. 4.5 Same as fig. 4.1, but all TurboMAP stations in 2011.
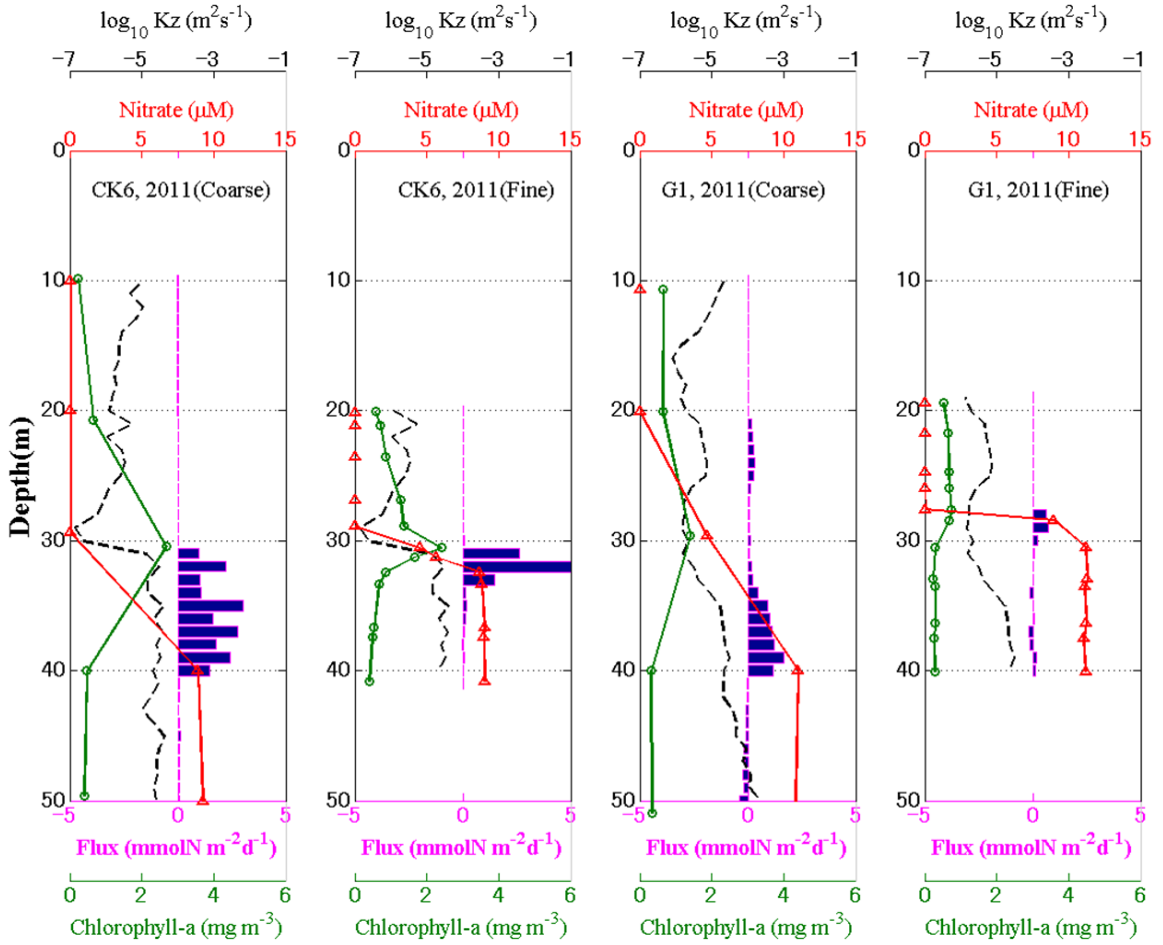
Fig. 4.6 Vertical profiles of vertical eddy diffusivity (Kz), nitrate concentration, chlorophyll a concentration, and the vertical nitrate flux in coarse and fine measurement structures at CK6 and G1, 2011, respectively. Vertical eddy diffusivity is plotted on a log scale.
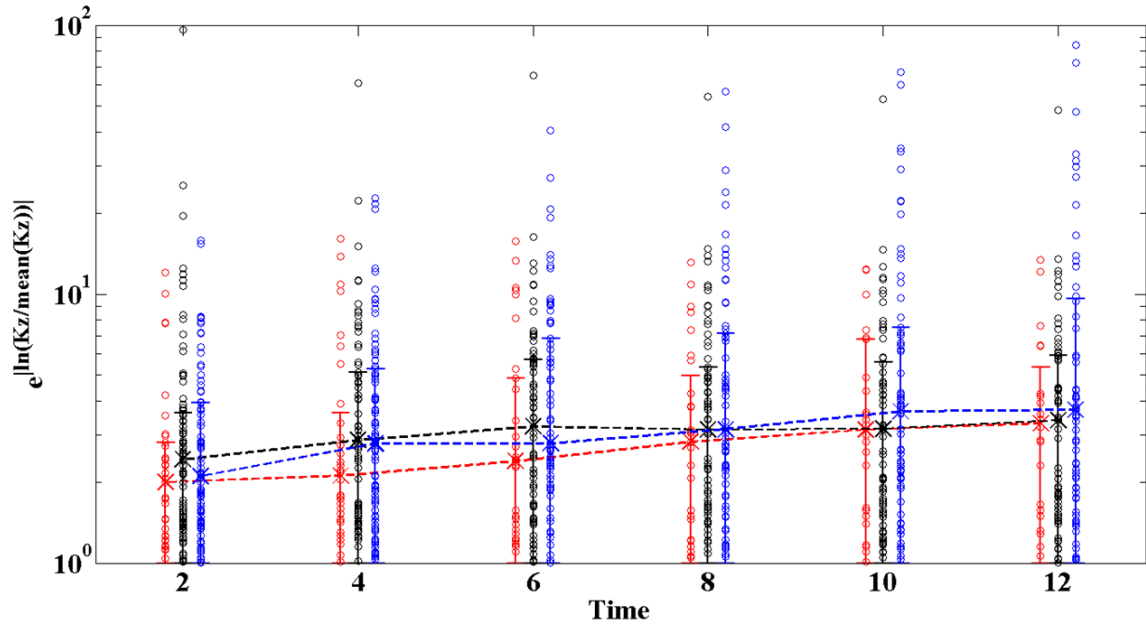
Fig. 4.7 The median (x marker), and 0% and 75 % quantiles of the relative ratio of the observed and mean vertical eddy diffusivity (*Kz*) within a fixed time interval in 2009 (red), 2010 (black) and 2011 (blue). The marker (o) shows the distribution of the relative ratio. The Y axis reflects the relative ratio between the observed and mean *Kz* (observed *Kz*/mean *Kz* when observed *Kz* > mean *Kz* and mean *Kz*/observed *Kz* when observed *Kz* < mean *Kz*).

5. Conclusion

Extensive observations including hydrology, water samplings, and turbulence measurements, were conducted on summer cruises during the period 2009−2011 in the continental shelf region of the northern ECS.

Nutrients used for new production were supplied from different sources and driving pathways of water mass in this area. Thereafter, the characteristic N/P ratio would change according to nutrient composition, and the N/P ratio could be an indicator originating from a unique water mass or nutrient source. Nitrate-rich water appeared occasionally due to the influence of CDW, even at the subsurface, and phosphate-rich water appeared due to the movement of the KSSW or subsurface water on the shelf. A relatively shallow SCM was located within the nitracline when the riverine input of nutrients was large, while a deep SCM was located slightly above the nitracline when the vertical supply of nutrients was large. The magnitudes of the nutrient flux caused by vertical mixing, vertical eddy diffusivity, and consequent contribution to IPPS were small, with a high N/P ratio within CDW expansion, whereas those were large, with a low N/P ratio, when the nutrient supply of KSSW was from the lower layer. A large diffusion flux accounted for most of the nutrient supply in the vicinity of the SCM resulting in LNP, while nutrients from CDW, supplied through horizontal advection are presumably used in the case of HNP. Considering the nutrient sources were unique to individual water masses, an approach based on the N/P ratio would suggest a clue for nutrient supply from the lower layer.

To compensate for the inconvenient comparison between turbulent flux and primary production with snapshot measurements, the variations in the nutrient flux and

primary production over 4 days were calculated from the time series measurements. Time series measurement showed a consistency about the large contribution of vertical nutrient flux to IPPS for LNP corresponding to snapshot measurement. This notable difference between the HNP and LNP fluxes was statistically significant. Because the difference is larger than the statistical range of Kz within which values from snapshot measurements. This study focused on quantifying nutrient flux caused by vertical mixing with direct turbulence measurements and comparing them with the consequent primary production in the vicinity of the SCM, which was obtained by simultaneous biological measurements. As a result, we conclude that nutrient flux caused by vertical mixing makes an important contribution to the supply of nutrients to the SCM, despite some uncertainties in estimating the nutrient flux and new production.

Acknowledgements

I would like to thank all the people who contributed in some way to the work described in this thesis.

First and foremost, my sincere gratitude goes to my supervisor T. Matsuno for his kind encouragement and patient supervision. I appreciate all his contributions of time, ideas, and funding to make my Ph.D. experience and adaptation of life in Japan. He always advised me when I am needed and gave me many chances to join in research cruise.

Prof. T. Senjyu is greatly thanked for valuable discussion, hearty encouragement and humor in lab meeting as well as examination of my thesis. I also thank the rest of my committee: Prof. A. Isobe, Prof. X. Guo for their guidance and encouragement to widen the understanding my research.

Dr. T. Endo and Dr. E. Tsutsumi are sincerely thanked for his helpful suggestions and discussions during the time we shared. I would also like to acknowledge the members of the OCD laboratory and other professors and staffs in the department of Earth System Science and Technology, and the Research Institute for Applied Mechanics in Kyushu University.

In particular, I appreciate Prof. J. Ishizaka for helping me approach the biological oceanography. Special thanks must be made to my collaborators: Dr. Y. Zhu, Prof. S. Takeda, and Dr. C. Sukigara who provided biochemical data and rendered their valuable time and effort to comment and review my research paper.

I appreciate all participants during the Nagasaki-maru cruises for joyful time and successful data collection. I also thank the captain, officers and crew of the Nagasaki-maru, training ship of the Faculty of Fisheries, Nagasaki University for their great assistance in the collecting data.

Finally, I am deeply indebted to my family for their love and support.

REFERENCES

Chang, J., Shiah, F. K., Gong, G. C., and Chiang, K. P. (2003), Cross-shelf variation in carbon-to-chlorophyll a ratios in the East China Sea, summer 1998. *Deep Sea Research Part II: Topical Studies in Oceanography*, 50(6), 1237-1247.

Chang, P.-H., and A. Isobe (2003), A numerical study on the Changjiang diluted water in the Yellow and East China Seas, *J. Geophys. Res.*, 108, 3299, doi:10.1029/2002JC001749, C9.

Chen, C. T. A., (1996), The Kuroshio intermediate water is the major source of nutrients on the East China Sea continental shelf. *Oceanologica Acta*, 19(5), 523-527.

Chen, C.T.A., and S.L. Wang, (1999), Carbon, alkalinity and nutrient budget on the East China Sea continental shelf, *J. Geophys. Res.*, 104, 20675-20686.

Chen, Y.-L., H.-B. Lu, F.-K. Shiah, G.-C. Gong, K.-K. Liu, and J. Kanda, (1999), New production and f-ratio on the continental shelf of the East China Sea: comparisons between nitrate inputs from the subsurface Kuroshio Current and the Changjiang River. *Estuarine, Coastal and Shelf Sci.*, 48, 59-75.

Chen, Y.-L., H.-Y. Chen, W.-H. Lee, C.-C. Hung, G.-T. Wong, and J. Kanda, (2001), New production in the East China Sea, comparison between well-mixed winter and stratified summer conditions, *Cont. Shelf Res.*, 21, 751-764.

Christian, J. R., and Karl, D. M., (1994), Microbial community structure at the US-Joint Global Ocean Flux Study Station ALOHA: Inverse methods for estimating biochemical indicator ratios. *Journal of Geophysical Research: Oceans*, 99(C7), 14269-14276.

Crawford W., and R. Dewey, (1989), Turbulence and mixing: sources of nutrients on the Vancouver Island continental shelf, *Atmosphere-Ocean*, 27, 428-442, doi:10.1080/07055900.1989.9649345.

Cullen, J. J., (1982), The deep chlorophyll maximum: comparing vertical profiles of chlorophyll a. *Canadian Journal of Fisheries and Aquatic Sciences*, 39(5), 791-803.

Edmond, J. M., A. Spivack, B. C. Grant, M. H. Hu, Z. X. Chen, S. Chen, and X. S. Zeng, (1985), Chemical dynamics of the Changjiang estuary, *Cont. Shelf Res.*, 4, 17-36.

Endoh, T., T. Matsuno, Y. Yoshikawa, and E. Tsutsumi, (2014), Estimates of the turbulent kinetic energy budget in the oceanic convective boundary layer. *J. Oceanogr.*, 70(1), 81-90.

Eppley, R.W., and E.H. Renger, (1986), Nitrate-based primary production in nutrient-depleted surface waters off California, *Oceanogr Trop*, 21(2), 229-238.

Fernand, L., Weston, K., Morris, T., Greenwood, N., Brown, J., and Jickells, T. (2013), The contribution of the deep chlorophyll maximum to primary production in a seasonally stratified shelf sea, the North Sea. *Biogeochemistry*, 113(1-3), 153-166.

Furuya, K., (1990), Subsurface chlorophyll maximum in the tropical and subtropical western Pacific Ocean: Vertical profiles of phytoplankton biomass and its relationship with chlorophylla and particulate organic carbon. *Marine Biology*, 107(3), 529-539.

Gong, G. C., Chen, Y. L. L., and Liu, K. K., (1996), Chemical hydrography and chlorophyll a distribution in the East China Sea in summer: implications in nutrient dynamics. *Con. Shelf Res.*, 16(12), 1561-1590.

Gong, G.-C., F.-K. Shiah, K.-K. Liu, Y.-H. Wen, and M.-H. Liang, (2000), Spatial and temporal variation of chlorophyll *a*, primary productivity and chemical hydrography in the southern East China Sea, *Cont. Shelf Res.*, 20, 411-436.

Gong G.-C., Y.-H. Wen, B.-W. Wang, and G.-J. Liu, (2003), Seasonal variation of chlorophyll a concentration, primary production and environmental conditions in the subtropical East China Sea, *Deep Sea Res II* 50(6–7), 1219-1236, doi:10.1016/S0967-0645(03)00019-5.

Hales, B., T. Takahashi, and L. Bandstra, (2005), Atmospheric CO_2 uptake by a coastal upwelling system, *Global Biogeochem. Cycles*, 19, GB1009, doi:10.1029/2004GB002295.

Hickman, A. E., Moore, C., Sharples, J., Lucas, M. I., Tilstone, G. H., Krivtsov, V., and
Holligan, P. M., (2012), Primary production and nitrate uptake within the seasonal
thermocline of a stratified shelf sea. *Marine Ecology Progress Series*.

Holligan, P. M., Williams, P. J. leB., Purdie, D., and Harris, RP, (1984), Photosynthesis,
respiration and nitrogen supply of plankton populations in stratified, frontal and
tidally mixed shelf waters. *Mar. Ecol. Prog. Ser*, 17, 201-213.

Holm-Hansen, O., and Hewes, C. D., (2004), Deep chlorophyll-a maxima (DCMs) in
Antarctic waters, *Polar Biol.*, 27(11), 699-710.

Isobe, A., and T. Matsuno, (2008), Long-distance nutrient-transport process in the
Changjiang river plume on the East China Sea shelf in summer, *J. Geophys. Res.*,
113, C04006, doi:10.1029/2007JC004248.

Kim, H., H. Yamaguchi, S. Yoo, J. Zhu, K. Okamura, Y. Kiyomoto, K. Tanaka, S.-W.
Kim, T. Park, I. S. Oh, and J. Ishizaka, (2009), Distribution of Changjiang Diluted
Water detected by satellite chlorophyll-a and its interannual variation during
1998-2007, *J.Oceanogr.*, 65 (1), 129-135.

Koronen, K., S. Hällfors, M. Kokkonen, and H. Kuosa, (1998), Development of a
subsurface chlorophyll maximum at the entrance to the Gulf of Finland, Baltic
Sea, *Limnol. Oceanogr.*, 43(6), 1089-1106.

Kwak, J.-H., J.-S. Hwang, E.-J. Choy, H.-J. Park, D.-J. Kang, T.-S. Lee, K.-I. Chang, K.-
R. Kim, and C.-K. Kang, (2013), High primary productivity and f-ratio in summer
in the Ulleung basin of the East/Japan Sea, *Deep-Sea Res. I*, 79, 74-85.

Lee, J. H., I. Lozovatsky, S.-T. Jang, C. J. Jang, C. S. Hong, and H. J. S. Fernando
(2006), Episodes of nonlinear internal waves in the northern East China Sea,
Geophys. Res. Lett., 33, L18601, doi:10.1029/2006GL027136.

Letelier, R. M., Karl, D. M., Abbott, M. R., and Bidigare, R. R., (2004), Light driven
seasonal patterns of chlorophyll and nitrate in the lower euphotic zone of the
North Pacific Subtropical Gyre, *Limnol. Oceanogr.*, 49(2), 508–519

Lewis, M. R., Harrison, W. G., Oakey, N. S., Herbert, D., and Platt, T., (1986), Vertical nitrate fluxes in the oligotrophic ocean, *Science(Washington)*, 234(4778), 870-872.

Lie, H.-J., C.-H. Cho, J.-H. Lee, and S. Lee, (2003), Structure and eastward extension of the Changjiang River plume in the East China Sea, *J. Geophys. Res.*, 108(C3), 3077, doi:10.1029/2001JC001194.

Liu, K.-K., S.-C. Pai, and C.-T. Liu, (1990), Temperature-nutrient relationships in the Kuroshio and adjacent waters near Taiwan, *Acta Oceanographica Taiwanica*, 21, 1-17.

Liu, K.-K., Tang, T.-Y., Gong, G.-C., Chen, L.-Y., Shiah, F.-K., (2000), Cross-shelf and along-shelf nutrient fluxes derived from flow fields and chemical hydrography observed in the southern East China Sea off northern Taiwan, *Cont. Shelf Res.*, 20 (4-5), 493-523.

Liu, K.-K., S.-Y. Chao, H.-J. Lee, G.-C. Gong, and Y.-C. Teng, (2010), Seasonal variation of primary productivity in the East China Sea: A numerical study based on coupled physical-biogeochemical model, *Deep-Sea Res. II*, 57, 1762-1782.

Liu, X., K. Furuya, T. Shiozaki, T. Masuda, T. Kodama, M. Sato, H. Kaneko, M. Nagasawa, and I. Yasuda, (2013), Variability in nitrogen sources for new production in the vicinity of the shelf edge of the East China Sea in summer, *Cont. Shelf Res.*, 61-62, 23-30.

Marra, J. F., (2014), Ocean productivity: A personal perspective since the first Liege Colloquium, *J. Mar. Syst.*, http://dx.doi.org/10.1016/j.jmarsys.2014.01.012.

Matsuno, T., M. Shimizu, Y. Morii, H. Nishida, and Y. Takaki, (2005), Measurements of the turbulent energy dissipation rate around the shelf break in the East China Sea, *J. Oceanogr.*, 61, 1029-1037, doi:10.1007/s1 0872-006-0019-9.

Matsuno, T., J.-S. Lee, M. Shimizu, S.-H. Kim, and I.-C. Pang, (2006), Measurements of the turbulent energy dissipation rate ε and an evaluation of the dispersion process of the Changjiang diluted water in the East China Sea, *J. Geophys. Res*, 111, C11S09, doi:10.1029/2005JC003196.

Matsuno, T., Lee, J.-S., and Yanao, S., (2009), The Kuroshio exchange with the South and East China Seas, *Ocean Sci.*, 5, 303-312, doi:10.5194/os-5-303-2009.

Matsuno, T., I.-S. Han, S.-H. Kim, I.-C. Pang, and J.-H. Lee, (2010a), Contribution of subsurface water to increase in salinity and satellite chlorophyll in the Changjiang Diluted Water, East China Sea, *Pacific Oceanogr.*, 5, 1, 19-30, Proc. 4th PEACE Ocean Science Workshop.

Matsuno,T., M. Shimizu, I.-C. Pang, S.-H. Kim, I.-S. Han, and K. Fukudome, (2010b), Behavior of Changjiang Diluted Water in the East China Sea, *Monitoring and Prediction of Marine and Atmospheric Environmental Change in the East Asia,* Ed. T.Yanagi, 21-32.

McGillicuddy, D. J., and A. R. Robinson, (1997), Eddy-induced nutrient supply and new production in the Sargasso Sea. *Deep Sea Research Part I: Oceanographic Research Papers*, 44(8), 1427-1450.

McGillicuddy, D. J., Robinson, A. R., Siegel, D. A., Jannasch, H. W., Johnson, R., Dickey, T. D., J. McNeil, A. F. Michaels, and Knap, A. H., (1998), Influence of mesoscale eddies on new production in the Sargasso Sea, *Nature*, 394(6690), 263-266.

McGowan, J. A., and Hayward, T. L., (1978), Mixing and oceanic productivity. *Deep Sea Research*, 25(9), 771-793.

Michaels, A.F., Knap, A.H., Dow, R.L., Gundersen, K., Johnson, R.J., Sorensen, J., Close, A., Knauer, G.A., Lohrenz, S.E., Asper, V.A. and Tuel, M., (1994), Seasonal patterns of ocean biogeochemistry at the US JGOFS Bermuda Atlantic Time-series Study site, *Deep Sea Research Part I: Oceanographic Research Papers*, 41(7), 1013-1038.

Mino, Y., S. Matsumura, T. Lirdwitayaprasit, T. Fujiki, T. Yanagi, and T. Saino, (2014), Variations in phytoplankton photo-physiology and productivity in a dynamic eutrophic ecosystem: a fast repetition rate fluorometer-based study. *J. Plankton Res.*, 36(2), 398-411.

Nasmyth, P. W., (1970), Oceanic turbulence, Ph.D. thesis, Institute of Oceanography, University of British Columbia, Vancouver, Canada, 69 pp.

Oakey, N. S., (1982), Determination of the rate of dissipation turbulent energy from simultaneous temperature and velocity shear microstructure measurements, *J. Phys. Oceanogr.*, 12, 256-271.

Omand, M. M., F. Feddersen, R. T. Guza, and P. J. S. Franks, (2012), Episodic vertical nutrient fluxes and nearshore phytoplankton blooms in Southern California, *Limnol. Oceanogr.*, 57(6), 1673-1688, doi:10.4319/lo.2012.57.6.1673.

Osborn, T. R., (1980), Estimates of the local rate of vertical diffusion from dissipation measurements, *J. Phys. Oceanogr.*, 10(1), 83-89.

Platt, T., C.L. Gallegos, and W.G. Harrison, (1980), Photoinhibition of photosynthesis in natural assemblages of marine phytoplankton, *J. Mar. Res.*, 38, 687-701.

Schafstall, J., M. Dengler, P. Brandt, and H. Bange, (2010), Tidal-induced mixing and diapycnal nutrient fluxes in the Mauritanian upwelling region, *J. Geophys. Res.*, 115, C10014, doi:10.1029/2009JC005940

Sharples, J., Tweddle, J. F., Mattias Green, J. A., Palmer, M. R., Kim, Y-N., Hickman, A. E., Holligan, P. M., Moore, C. M., Rippeth, T. P., Simpson, and J. H., Krivtsov, V., (2007), Spring-neap modulation of internal tide mixing and vertical nitrate fluxes at a shelf edge in summer. *Limnol. Oceanogr.*, 52 (5). 1735-1747, doi:10.4319/lo.2007.52.5.1735.

Shiozaki, T., K. Furuya, H. Kurotori, T. Kodama, S. Takeda, T. Endoh, Y. Yoshikawa, J. Ishizaka, and T. Matsuno, (2011), Imbalance between vertical nitrate flux and nitrate assimilation on a continental shelf: Implications of nitrification, *J. Geophys. Res.*, 116, C10031, doi:10.1029/2010JC006934.

Siswanto, E., J. Ishizaka, K. Yokouchi, K. Tanaka, K.Okamura, A. Kristijono, and T. Saino, (2008), Ocean physical and biogeochemical responses to the passage of Typhoon Meari in the East China Sea observed from Argo float and multiplatform satellites, *Geophys. Res. Lett.*, 35, L15604, doi:10.1029/2008GL035040.

Umezawa, Y., Yamaguchi A., Ishizaka J., Hasegawa T., Yoshimizu C., Tayasu I.,Yoshimura H., Morii Y., Aoshima T., and Yamawaki N., (2014), Seasonal shifts in the contributions of the Changjiang River and the Kuroshio Current to nitrate dynamics in the continental shelf of the northern East China Sea based on a nitrate dual isotopic composition approach. *Biogeosciences*, 11.4: 1297-1317.

Venrick, E. L., (1993), Phytoplankton seasonality in the central North Pacific: the endless summer reconsidered, *Limnol. Oceanogr.*, 38(6), 1135-1149.

Williams, C., J. Sharples, M. Green, C. Mahaffey, and T. Rippeth, (2013), The maintenance of the subsurface chlorophyll maximum in the stratified western Irish Sea, *Limnol. Oceanogr.*: Fluids and Environments, 3, 61-73.

Yoon, J. E., J. Park, S. Yoo, (2012), Comparison of primary productivity algorithms for Korean waters, *Ocean Science Journal*, 47(4), 473-487.

Zhang, J., (1996), Nutrient elements in large Chinese estuaries, *Cont. Shelf Res.*, 16, 1023-1045.